



Yago Chamoun Ferreira Soares

**Rheological behavior of graphene oxide suspensions
in poly(ethylene glycol)**

Dissertação de Mestrado

Dissertation presented to the Programa de Pós-graduação em Engenharia Mecânica of PUC-Rio in partial fulfillment of the requirements for the degree of Mestre em Engenharia Mecânica.

Advisor: Prof^a. Mônica Feijó Naccache
Co-advisor: Prof. Ricardo Jorge Espanhol Andrade

Rio de Janeiro
October 2019



Yago Chamoun Ferreira Soares

**Rheological behavior of graphene oxide suspensions
in poly(ethylene glycol)**

Dissertation presented to the Programa de Pós-graduação em Engenharia Mecânica of PUC-Rio in partial fulfillment of the requirements for the degree of Mestre em Engenharia Mecânica. Approved by the Examination Committee.

Prof^a. Mônica Feijó Naccache

Advisor

Departamento de Engenharia Mecânica – PUC-Rio

Prof. Ricardo Jorge Espanhol Andrade

Co-advisor

Mackenzie

Prof. Roney Leon Thompson

UFRJ

Prof. Aurora Pérez Gramatges

Departamento de Química – PUC-Rio

Rio de Janeiro, October 4th, 2019

All rights reserved.

Yago Chamoun Ferreira Soares

The author holds a bachelor's degree in petroleum engineering from the Universidade Federal Fluminense in 2017. He has participated in several national and international congresses presenting his articles. In the master's degree, developed research in the field of thermoscience focusing on rheological characterization of non-Newtonian fluids.

Bibliographic data

Soares, Yago Chamoun Ferreira

Rheological behavior of graphene oxide suspensions in poly (ethylene glycol) / Yago Chamoun Ferreira Soares; advisor: Mônica Feijó Naccache; co-advisor: Ricardo Jorge Espanhol Andrade. – 2019. 103 f. : il. color. ; 30 cm

Dissertação (mestrado)—Pontifícia Universidade Católica do Rio de Janeiro, Departamento de Engenharia Mecânica, 2019.
Inclui bibliografia

1. Engenharia Mecânica – Teses. 2. Comportamento reológico. 3. Óxido de grafeno. 4. Polietileno glicol. 5. Técnicas de caracterização. I. Naccache, Mônica Feijó. II. Andrade, Ricardo Jorge Espanhol. III. Pontifícia Universidade Católica do Rio de Janeiro. Departamento de Engenharia Mecânica. IV. Título.

CDD: 621

I dedicate this work to my parents who gave me so much support and encourage to do this master's degree in the best way possible, giving me the free will to opt for this course and which way to follow in a way that allowed me to work with peace and tranquility so that everything flowed naturally and leaving me the will to execute not only this project that demands a lot of work and dedication, but also the other necessary subjects for my academic formation.

Acknowledgments

First of all, I thank God for having given me wisdom and family with financial conditions to study my studies so that I could have a good base and be able to pass to the Pontifical Catholic University which is a college of excellent academic level.

Thanks also to my parents for the incentives and psychological and financial support so that I could successfully obtain the Master's degree in Mechanical Engineering.

To my mentor Mônica Feijó Naccache and my co-advisor Ricardo Jorge Espanhol Andrade for their support in the preparation of this work and for the learning they provided me with a topic of extremely high international importance.

To Eyff Cargnin, Mackenzie-SP student, who was very important for the development of this work providing me with all the necessary support.

To my friends, not only from college, but from all of life, who always encouraged me to choose what I wanted and always being on my side supporting the good and bad moments of my life.

This study was financed in part by the Coordenação de Aperfeiçoamento de Pessoal de Nível Superior - Brasil (CAPES) - Finance Code 001.

Abstract

Soares, Yago Chamoun Ferreira; Naccache, Mônica Feijó (Advisor); Andrade, Ricardo Jorge Espanhol (Co-advisor). **Rheological behavior of graphene oxide suspensions in poly(ethylene glycol)**. Rio de Janeiro, 2019. 103p. Dissertação de Mestrado – Departamento de Engenharia Mecânica, Pontifícia Universidade Católica do Rio de Janeiro.

Graphene is formed by a monolayer of carbon atoms linked together forming a hexagonal network. It has been extensively studied by researchers and attracted investment from various sectors of the economy, because it presents excellent mechanical, thermal, electrical and optical properties. The present work has as main objective the rheological characterization of the suspensions of graphene oxide (GO) dispersed in poly(ethylene) glycol (PEG 400), with different oxidation times (2 and 96 hours), through the use of rotational rheometry. Graphene oxide was obtained by Hummers method and characterized by various techniques. This method is based on the chemical exfoliation of graphite using strong acids such as sulfuric acid. Once the graphite oxide (GrO) is obtained, it is exfoliated in an ultrasonic bath in PEG to form the suspension with graphene oxide. The rheological characterization is fulfilled through measurements in steady shear flow, transient shear flow and oscillatory shear flow. The characterization of GO was performed using techniques such as: X-Ray Diffraction (XRD), Raman Spectroscopy, Fourier Transform Infrared (FTIR), Atomic Force Microscopy (AFM) and Thermogravimetric Analysis (TGA). The results will serve as a basis for understanding the interaction between the GO and the polymer, and the rheological behavior of GO-based polymer nanofluids.

Keywords

Rheological behavior; graphene oxide; polyethylene glycol; techniques characterization.

Resumo

Soares, Yago Chamoun Ferreira; Naccache, Mônica Feijó; Andrade, Ricardo Jorge Espanhol. **Comportamento reológico de suspensões de óxido de grafeno em polietileno glicol**. Rio de Janeiro, 2019. 103p. Dissertação de Mestrado – Departamento de Engenharia Mecânica, Pontifícia Universidade Católica do Rio de Janeiro.

O grafeno é formado por uma monocamada de átomos de carbono ligados entre si formando uma rede hexagonal. Ele tem sido bastante estudado por pesquisadores e atraído investimentos de vários setores da economia por apresentar excelentes propriedades mecânicas, térmicas, elétricas e ópticas. O presente trabalho tem como objetivo principal a caracterização reológica das suspensões de óxido de grafeno (GO) dispersas em polietileno glicol (PEG 400), com diferentes tempos de oxidação (2 e 96 horas), através do uso da reometria rotacional. O óxido de grafeno foi obtido pelo método de Hummers e caracterizado por várias técnicas. Este método é baseado na esfoliação química do grafite através de ácidos fortes, como o ácido sulfúrico. Uma vez que o óxido de grafite (GrO) é obtido, ele é esfoliado em um banho ultrassônico em PEG para a formação da suspensão com óxido de grafeno. A caracterização reológica foi realizada através de medições em escoamento de cisalhamento em regime permanente, transiente e oscilatório. A caracterização do GO foi realizada utilizando técnicas como: Difração de Raios-X (DRX), Espectroscopia Raman, Infravermelho por Transformada de Fourier (FTIR), Microscopia de Força Atômica (AFM) e Análise Termogravimétrica (TGA). Os resultados servirão de base para a compreensão da interação entre o GO e o polímero, e o comportamento reológico dos nanofluidos de polímeros à base de GO.

Palavras-chave

Comportamento reológico; óxido de grafeno; polietileno glicol; técnicas de caracterização.

Summary

1. INTRODUCTION	17
1.1. Objectives	21
1.1.1. Specific objectives	21
1.2. Justification and relevance of the study	22
1.3. Organization of the manuscript	22
2. IMPORTANT CONCEPTS IN RHEOLOGY	24
3. LITERATURE REVIEW	32
3.1 Nanotechnonology	32
3.2 Nanofluids	34
3.3. Carbon alotropes and its oxygenated derivatives	38
3.3.1. Graphite	40
3.3.2. Graphite oxide	41
3.3.3. Graphene oxide	42
3.3.4. Graphene	44
3.3.5. Methods of obtaining graphene	47
3.4 Poly(ethyelene) glycol	51
3.5 Previous Works	52
4. CHARACTERIZATION TECHNIQUES	54
4.1. X-Ray Diffraction (XRD)	54
4.2 Raman Spectroscopy	55
4.3. Thermogravimetric Analysis (TGA)	56
4.4. Atomic Force Microscopy (AFM)	58
4.5. Infrared Vibrational Spectroscopy (FTIR)	59
5. MATERIALS AND METHODS	60
5.1. Materials	60
5.2. Sample preparation method	61
5.3. Characterization	64
5.4. Rheological measurements	65
6. RESULTS AND DISCUSSIONS	69

6.1. Structure characterization of graphene oxide	69
6.1.1. X-Ray Diffraction (XRD).....	69
6.1.2 Raman Spectroscopy	71
6.1.3. Thermogravimetric Analysis (TGA)	72
6.1.4. Atomic Force Microscopy (AFM).....	75
6.1.5. Infrared Vibrational Spectroscopy (FTIR)	77
6.2. Rheology of graphene oxide suspensions in poly(ethylene) glycol	79
 7. CONCLUSIONS	 95
 8. REFERENCES	 97

List of figures

Figure 1.1 – Carbon-based structures. (Zarbin and Oliveira, 2013).....	18
Figure 1.2 – Representation of the probable functional groups present in the structure of graphene oxide (Ma, 2017)	19
Figura 2.1 – Plots of shear stress versus shear rate for non-Newtonian and Newtonian fluids: a. time-independent b. time-dependent fluids. (Jaluria, 2001)	28
Figura 2.2 – Flow curve of: a. time-independent and b. time-dependent fluids (Richardson, 2011)	28
Figure 2.3 – Schematic diagram of basic tool geometries for the rotational rheometer: (a) concentric cylinders (couette), (b) cone-plate, (c) parallel plates and (d) double-gap	30
Figure 3.1 – Carbon Nanotube Nanofluids in 10nm, 300nm, and 500nm Distinct Scale Images (Hosokawa et al., 2007).....	34
Figure 3.2 – Scheme of the high pressure homogenizer for the production of nanofluids (Hwang et al., 2008)	35
Figure 3.3 – Commom challenges of nanofluid development (Taha-Tijerina, 2018)	36
Figure 3.4 – Scheme of nanoparticles sedimentation over time (Taha-Tijerina, 2018).....	37
Figure 3.5 – Brownian motion of the particle (Das, 2017).....	38
Figure 3.6 – Carbon Allotropes: a) 2-D graphene, b) Fullerene, c) Carbon nanotube d) 3-D grafite (Phiri et al., 2017).....	39
Figure 3.7 – Hybridization state of some carbon allotropes (adapted from Negreti, 2016).....	40
Figure 3.8 – Schematic representation of the graphite oxidation reaction (Sampaio, 2017).....	41
Figure 3.9 – Graphene hexagonal crystal structure representation (hypescience, 2014)	44
Figure 3.10 – Graphene production scheme by bottom-up and top-down (Maraschin, 2016).....	44
Figure 3.11 – Top-down Process Schemes (adapted from Camargos e Silva, 2017)	46
Figure 3.12 – Schematic illustration of GO preparation process (Ma, 2017).....	48
Figure 3.13 – Examples of models presented for the graphene oxide structure proposed by: a) Hofmann b) Ruess c) Sholz e Boehm d) Nakajima e Matsuo e) Dékany f) Ajayan g) Lerf e Klinowski (Cardoso, 2015).....	49

Figure 3.14 – Schematic structure of reduced graphene oxide (Griggs and Medina, 2016).....	50
Figure 3.15 – Partial planar representation of the PEG molecule with the available sites for interactions with the other components of the system (Santos, 2011).....	51
Figure 4.1 – Experimental tool used for the application of the X-Ray Diffraction technique (XRD)	55
Figure 4.2 – Raman Spectrometer (IMC Laboratory of Raman spectroscopy of the University of Caxias do Sul).....	56
Figura 4.3 – Apparatus used to perform TGA.....	57
Figura 4.4 – TGA measurement of the oxidation of natural graphite in air. Heating rate 10°C/min (Jiang et al., 2010)	57
Figura 4.5 – microscope used for the characterization by AFM	58
Figure 4.6 – FTIR Spectrometer (Itscientific.com/product/vertex-7070v-ftir-research-spectrometers).....	59
Figure 4.7 – Graphite FTIR spectrum (Kartick, 2013).....	59
Figure 5.1 – Some laboratory equipment were used to obtain GO through the modified hummers method.....	61
Figure 5.2 – Reaction among graphite, sulfuric acid and potassium permanganate under low temperature and agitation	62
Figure 5.3 – The generated product being filtered with a vacuum pump.....	63
Figure 5.4 – The final product being macerated.....	63
Figure 5.5 – The colloidal suspensions being exfoliated in an ultrasonic bath	64
Figure 5.6 – The suspensions being stirred on magnet stirrer	65
Figure 5.7 – (a) smooth cone-plate separately and (b) cone-plate coupled to the rheometer.....	67
Figure 5.8 – (a) the geometry of double-gap separately (b) the top and bottom cylinder coupled together	67
Figure 6.1 – XRD interference planes for (a) GO 96h (b) GO 2h and (c) Graphite	70
Figure 6.2 – Raman spectrum of the (a) GO 96h (b) GO 2h and (c) Graphite.....	72
Figure 6.3 – Thermogravimetric curves for (a) GO-2h and (b) GO-96h oxidized	75
Figure 6.4 – Frequency (%) of GO sheets of (a) 2h and (b) 96h of oxidation as function of their height	76
Figure 6.5 – FTIR spectrum of GO with (a) 2h (b) 96h of oxidation.....	78
Figure 6.6 – Flow Curve of aqueous dispersion with 10mg/ml of GO-2h.....	79
Figure 6.7 – Stability tests for suspensions with concentrations of (a) 0.1 (b) 1 (c) 10 (d) 20 (e) 40 and (f) 80mg/ml of GO-2h comparing suspensions with agitation (filled symbols) and without agitation (open symbols)	81

Figure 6.8 – Pre-shear of GO-2h suspensions in polyethylene glycol with (a) 0.1 (b) 1 (c) 10 (d) 20 (e) 40 and (f) 80mg/mL	83
Figure 6.9 – Flow curve applying a shear rate of 10 to 1000s ⁻¹ (without pre-shearing the sample) and then 1000 to 10s ⁻¹ for suspensions with concentrations of (a) 0.1 (b) 1 (c) 10 (d) 20 (e) 40 and (f) 80mg/mL of GO-2h	84
Figure 6.10 – Flow curve comparing viscosity for suspensions with 40mg/mL of GO with different oxidation time	85
Figure 6.11 – Bridging effect (Wang et. al., 2012).....	86
Figure 6.12 – Shear viscosity of suspensions of GO as a function of different GO concentrations at shear rate 10s ⁻¹	87
Figure 6.13 – Schematic representation of the breakdown of the structure into flocs, with decreasing sizes as the shear rates increase (adapted from Vallés et al., 2014).....	88
Figure 6.14 – Steady shear rate flow behavior of the (a) GO of 2h (b) GO of 96h of oxidation.....	89
Figure 6.15 – Strain Sweep for (a) GO of 2h (b) GO of 96h of oxidation	92
Figure 6.16 – Frequency Sweep for (a) GO of 2h (b) GO of 96h of oxidation....	93
Figure 6.17 – Comparison of viscous and elastic modulus between suspensions with 40mg/mL of GO made with 2h and 96h of oxidation	94

List of tables

Table 3.1 – Physical and Chemical Properties of Some Allotropic Forms of Carbon (adapted from Valim, 2015)	39
Table 3.2 – Bottom-Up Processes for Graphene Synthesis (Negreti, 2016)	45
Table 5.1 – Products, reagents and the supplier company for the graphene oxide production)	60

List of Symbols and Abbreviations

CVD - Chemical Vapor Deposition

XRD - X-Ray Diffraction

PEG – Poly(ethylene) Glycol

FTIR – Fourier Transform Infrared

AFM – Atomic Force Microscopy

TGA – Thermogravimetric Analysis

GO – Graphene Oxide

GrO – Graphite Oxide

rGO – Reduced Graphene Oxide

SEM – Scanning Electron Microscopy

STM – Scanning Tunneling Microscope

PEO – Poly(ethylene oxide)

G' – Storage Modulus

G'' – Lost Modulus

De – Deborah Number

τ_y – Yield Stress

ClO₂ – Chlorine Dioxide

FDA – Food and Drug Administration

ω – Angular Frequency

γ_o – Strain Amplitude

δ – Phase Angle

σ_o – Amplitude of the Stress

H₂SO₄ – Sulfuric Acid

KMnO₄ – Potassium Permanganate

HCl – Hydrochloric Acid

H₂O₂ – Hydrogen Peroxide

C₂H₅OH – Ethanol

SiO₂ – Silicon Oxide

LVR – Linear Viscoelasticity Region

Al₂O₃ - Aluminum Oxide

Å – Angstroms

mGO – Multilayers Graphene Oxide

SAOS – Small Amplitude Oscillatory Shear

\emptyset – Concentration

\emptyset_c – critical concentration

“Não pretendemos que as coisas mudem, se sempre fazemos o mesmo. A crise é a melhor benção que pode ocorrer com as pessoas e países, porque a crise traz progressos. A criatividade nasce da angústia, como o dia nasce da noite escura. É na crise que nascem as invenções, os descobrimentos e as grandes estratégias. Quem supera a crise, supera a si mesmo sem ficar ‘superado’. Quem atribui à crise seus fracassos e penúrias, violenta seu próprio talento e respeita mais os problemas do que as soluções. A verdadeira crise é a crise da incompetência... Sem crise não há desafios; sem desafios, a vida é uma rotina, uma lenta agonia. Sem crise não há mérito. É na crise que se aflora o melhor de cada um...”

Albert Einstein

1

INTRODUCTION

Nanotechnology marked the evolution of a new scientific area in recent years by the simple fact that the properties of the materials also depend on its shape and size and not only on its composition and structure. Such technology can be applied in several scientific areas such as physics, mathematics, medicine, communication, among many other areas where it has great prominence (Bordoni, 2014).

Nanometric particles, when compared to the same materials at larger scales, have unique physical and chemical properties and the manufacture of these materials has been allowed due to new technologies that have emerged (Yu et al., 2007).

Among the variety of the most researched materials between academic papers and industries, we have polymer solutions reinforced with nanometric scale loads, with emphasis on carbon-based materials. The interest behind studying these materials also called nanofluids is due to the fact they tend to have better properties when compared with conventional suspensions. The properties of the material are reinforced, since they have a higher interaction between matrix/reinforcement when it comes to nanometric scale (Botan, 2011).

According to Witharama (2003), nanofluid is defined as a suspension of nanometer-sized particles (from 1 to 100 nm) in a base-fluid and this concept emerges from the field of nanotechnology. Several materials such as ceramic oxides, metal oxides (CuO, ZnO, TiO₂, SiO₂), metals (Cu, Ag, Au, Fe), carbon nanotubes (single and multiple wall) and graphene are used for the production of nanofluids (Oliveira, 2014).

Dynamic viscosity, thermal conductivity and specific heat are considered the main thermophysical properties of nanofluids and their determination depends not only on the base fluid used, but also on the particles that make up this fluid. And some of the factors that may interfere on these properties are volumetric concentration, particle size, morphology (size, shape, fractal surface), additives employed, production form, pH, among others (Noble, 2017).

In 2004, two Russian researchers discovered graphene through a simple process of exfoliation: using a duct tape, they wore a graphite plate out until obtain the

graphene. Graphene is a flat monolayer composed of carbon atoms with sp^2 hybridization linked together, forming a two-dimensional network. Besides being an extremely resistant material, flexible, impermeable and with thermal conductivity a thousand times greater than the one of copper, according to Vianna (2017), the material also presents high mobility of loads, optical transparency, vast superficial area and flexibility, combined with an enormous mechanical robustness and environmental stability. Figure 1 shows several crystalline structures composed of carbon atoms with sp^2 hybridization, which are: a) Graphite; b) diamond; c) fullerene; d) single-walled carbon nanotube; e) multiple wall carbon nanotube; f) graphene.

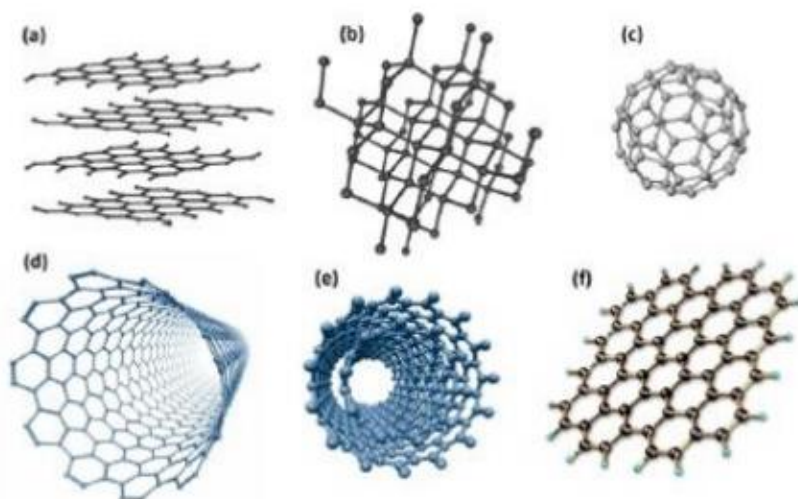


Figure 1.1- Carbon-based structures. (Zarbin and Oliveira, 2013)

Some carbon allotropes are rolled sheets of graphene, such as fullerene and carbon nanotubes, which are shaped like a sphere and a cylinder, respectively, while the graphite is a combination of graphene sheets organized alternately.

Graphene has been widely applied in recent years in polymer suspensions. This application can lead to increased electrical and thermal conductivity, mechanical and chemical resistance and improved thermal properties. Graphene, in the area of energy, can also be applied as an electron carrier layer in solar cells increasing its efficiency, or even being used in flexible supercapacitors with very high performance (Zarbin and Oliveira, 2013). In the area of biotechnology, it is used in phototherapy applications, biosensors for the prevention of diseases like cancer and

for composites with bacterial action, but can also be used in paints to increase resistance, in catalysts because it has a large contact area and even for purification and decontamination of water, among many other applications.

The method of exfoliation of graphite discovered in 2004, despite producing samples with a good structural quality, becomes impractical because it has no yield. And as an alternative to large scale production, there's the method is based on the chemical oxidation of graphite (the oxidation time variant can also be considered) forming the so-called graphene oxide (GO), which has epoxy and hydroxyl groups that when dispersed in water, present an antiphilic character. The edges of its predominantly hydrophilic structure occur as a result of the presence of functional groups containing oxygen and its plane hydrophobic composed of carbon atoms. In the figure below it is possible to observe the representation of a molecule of graphene oxide.

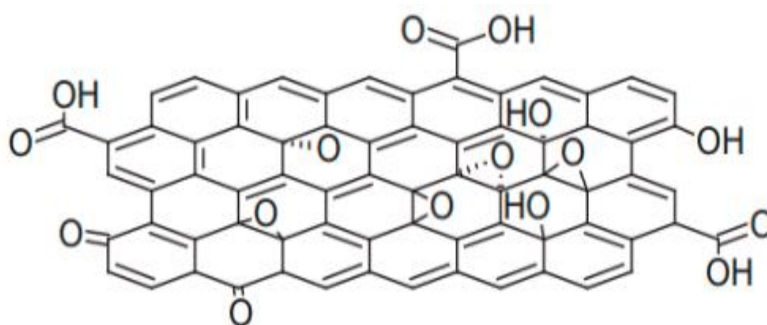


Figure 1.2 – Representation of the probable functional groups present in the structure of graphene oxide (Ma, 2017)

The GO, being hydrophilic, is capable of forming colloidal suspensions in a dispersing medium. Colloids are systems in which the component of one of its phases has nanometric dimensions (Ferreira and Silva, 2018). In the study, GO is the dispersed phase and PEG is the continuous phase of suspension.

There are two main methods of achieving high efficiency GO, even after years of intense study on this material: the Hummers and Staudenmaier method. They are based on the chemical exfoliation of graphite through attacks with strong acids, mainly sulfuric acid and nitric acid (Valim, 2015).

Graphene oxide is the most targeted material to be explored in the future with a gigantic potential market for the next years. This material has some advantages over graphene, such as better solubility and stability in aqueous media, due to oxidation converts the particles from hydrophobic to hydrophilic (Wick et al., 2014; Imperiali et al., 2012).

From the 21st century, researchers and scientists have begun to carry out measurements and tests with graphene suspensions and until nowadays few studies have been carried out on the rheological properties of these suspensions, although there are many articles that deal with the thermal and electrical properties of these nanofluids (Giudice and Shen, 2017).

Rheological properties are important to study because their knowledge helps in the design of pumps and pipes, agitators, heat exchangers, homogenizers, etc. It also helps in the quality control of the product (intermediate and final), checking the expiration date (foods, cosmetics) and determining properties of fluids such as blood to how it flows in of our veins / arteries, oils of different specifications used to lubricate engines, among other possible materials that can be used as objects of study. Therefore, it is possible to highlight the importance of knowledge of rheology for application in the most diverse industrial segments such as cosmetics, food, polymers, petroleum, paints, pharmaceuticals, personal hygiene, among others.

In the area of nanotechnology, the determination of the polymer in which GO will be applied after obtaining the charge of nanofluid is quite important. The present work studies the incorporation of GO in polyethylene glycol with molecular weight (M_w) of 400g / mol (PEG 400). PEG, in generally, is a water-soluble nonionic polymer, but PEG 400 is a liquid polymer and which is used as a kind of model polymer that has facility to interact with nanoparticles and it would assist in the study of GO with different oxidation levels. Futhermore, although not the main reason for this work, this polymer is very important for the pharmaceutical industry, especially nowadays, for the newer controlled drug release systems. It has also been widely used in several sectors, among them, the cosmetic and the dental area by virtue of its fantastic chemical properties.

The behavior of a polymeric material can be divided into two regimens: linear and non-linear viscosity. In the linear viscosity regime, the rheological behavior is modeled at slow and small deformations, so that the molecules do not leave their equilibrium state, thus allowing the characterization of this material at the structural level. However, with regard to the nonlinear viscosity regime, rheological behavior is modeled at faster and larger deformations, and it is possible to understand the behavior of the material. For either any of these two regime types, the materials can be subjected to an elongational or shear flow.

1.1 OBJECTIVES

The main objectives of this work are to evaluate the oxidation of the graphene oxide (GO) and analyse its effect on the rheological properties of the suspensions of GO dispersed in poly(ethylene) glycol (PEG). The rheological characterization is fulfilled through measurements in shear flow, mainly in steady and transient oscillatory regimes.

1.1.1 Specific objectives

- Prepare graphene oxide from chemical exfoliation of graphite using the modified Hummers method.
- Produce nanofluid composed of polyethylene glycol reinforced with graphene oxide.
- Evaluate rheological parameters for the characterization of the suspension through flow curves and oscillatory measurements.
- Characterization of the GO obtained through the techniques of X-Ray Diffraction (XRD), Raman Spectroscopy, Fourier Transform Infrared (FTIR), Atomic Force Microscopy (AFM) and Thermogravimetric Analysis (TGA) in order to evaluate its quality.
- Analyze the different rheological behavior and characterizations obtained for graphene oxides with different oxidation times (2 and 96 hours).

1.2 JUSTIFICATION AND RELEVANCE OF THE STUDY

The success in commercial applications of nanomaterials is related to the ability to produce high quality materials on an industrially viable scale when compared to those usually produced on a larger scale, and when applied to polymers, suspensions or emulsions, for example, these nanomaterials like graphene oxide tend to improve their properties.

Although graphene has excellent properties and many industrial applications, there is a big technological challenge to obtain it in large amounts, and with a low cost of production. There is a great deal of interest in developing preparation routes that are practically feasible with high yield and purity and good structural quality (Mehl et al., 2014). Nowadays, two possible alternatives are being applied: the first one that is called bottom-up, which is allied to the synthesis/production of the material; and the second, topdown, where the material is fragmented until it arrives in the wanted scale (Fim, 2012).

The most promising approach to produce graphene on a large scale in ourdays, it is to from graphite through chemical methods. This can result in the rapid development of new technologies and subsequent introduction into the market (Chua, 2014; Castrillón, 2015).

Numerous operations in the industries use complex fluids with non-Newtonian behavior. Non-Newtonian fluids are important for technological advancement in many sectors and therefore should be studied and understood so that their applicability in the market increases. Regarding the rheological characterization, the complete study of the mechanical behavior and the nature of each of these fluids, as in the present case is the suspension of polyethylene glycol with graphene oxide, it is necessary in order to determine its applications in certain procedures and to be able to evaluate and improve their properties, thus optimizing the processes where they are inserted.

Because of their excellent electrical, mechanical properties and thermal stability, many researchers have been interested in studying graphene/polymer nanocomposites, although they face some challenges during their processing such as the homogeneous dispersion of graphene in the polymer matrix (Shu et al., 2016). Up to now, studies have been conducted on the rheological behavior of graphene/polymer nanocomposites focusing on graphene processed from graphene oxide (GO) dispersed in some common solvents such as water. However, there are

few reports that aimed at the study of obtaining graphene oxide dispersed directly in a liquid polymeric matrix, as will be the focus of this work.

The amount of oxygenated functional groups that are inserted into the graphite structure is what determines the oxidation level of graphene oxide. Some factors such as the oxidation method, the graphite purity, the oxidizing agent used and the amount added, the reaction time are able to influence the degree of oxidation during GO synthesis. The degree of oxidation influences its morphology and GO properties. The size of graphene oxide sheets is related to the amount of C-O groups inserted in the structure, and the size of the GO is fundamental to determine its applications (Ferreira and Silva, 2018).

In the present study, the influence of different oxidation levels of GO on a model polymer (PEG 400) and the effects of GO concentrations were investigated, because it is necessary to investigate the rheological behavior of GO suspensions in some polymer once the polymeric matrix has a rheological response dependent on the particle-particle interactions with the polymer chain, so that it is possible to understand the effect in flow processes, that is, during industrial processes.

1.3 ORGANIZATION OF THE MANUSCRIPT

This text is divided in seven chapters. Chapter 1 presents an introduction of the work, the objectives and how it was structured. In chapter 2 the important concepts in rheology is presented. In Chapter 3 it is presented a literature review regarding the areas of study required for the development of the research. The characterization techniques and their mode of operation are presented in chapter 4. Chapter 5 describes the materials used, the methods for obtaining the graphene oxide, and the techniques and methodology used for the characterization of the graphene oxide and of the suspensions. The experimental results are presented in chapter 6. Chapter 7 shows conclusions obtained through the case study done in this work, and suggestions for future works.

2

IMPORTANT CONCEPTS IN RHEOLOGY

Rheology is the branch of science responsible for studying the flow of matter and the deformational behavior of materials when subjected to stresses during a certain period and under certain thermodynamic conditions. It is important to study this area of science because the rheological properties affect all phases of material in various sectors (from the development and stability of the formulation to the processing and performance of the product) and its knowledge helps in the design of pumps and pipes, agitators, heat exchangers, homogenizers, etc. It also helps in the quality control of the products (intermediate and final), checking the expiration date (foods, cosmetics) and determining properties of fluids such as blood to how it flows in of our veins / arteries, oils of different specifications used to lubricate engines, among other possible materials that can be used as objects of study. Therefore, it is possible to highlight the importance of these rheology techniques for application in the most diverse industrial segments such as cosmetics, food, polymers, petroleum, paints, pharmaceuticals, personal hygiene, among others.

According to Vasquez (2007), the materials generally present three types of behavior: viscous, elastic and viscoelastic. Viscosity is a rheological parameter that measures the ability of a material to resist flow, while elasticity represents the ability of a material to store deformational energy, that is, the ability of a material to return to its place of "comfort" after suffering disturbance. These types of behavior are observed when a material undergoes of deformation through an applied force. This deformational force is expressed as the stress, or force per unit area. The degree of deformation applied to a material is called the strain. Strain can also be expressed as sample displacement (after deformation) relative to the pre-deformation sample dimensions.

Viscoelastic materials present an intermediate mechanical behavior between the Hookean behavior of an elastic solid and Newtonian behavior of a viscous fluid, that is, they have an ability to dissipate deformational energy through the flow and to regain its original shape after being deformed, so that this material can be said to have a characteristic relaxation time. In the viscoelastic fluids there is a parameter that corresponds to the ratio of a relaxation time of the material (time required for some molecular movement) for a characteristic time of the deformation process (time of the experiment) known as the Deborah number (De). This Deborah number

corresponds to the relationship between the elastic and viscous forces of the material and allows the classification of a solid or liquid material (Barnes et al., 1989).

When the relaxation time of a material is extremely large tending to infinity or when the time of the deformation process is very fast it is possible to conclude that this process has characteristics of an elastic solid. However, when the relaxation time is extremely small or the time of the deformation process takes a long time to occur, this material presents characteristics of a viscous fluid. Polymeric materials have $0 < De < \infty$ and the values of the relaxation time depend on their molecular mass (Bretas and D'Ávila, 2000).

The deformation of a solid may be characterized by laws which describe the change in volume, size or shape, whereas the flow of a fluid which may be in the gaseous or liquid state, is characterized by laws which describe the continuous variation of the rate or degree deformation as a function of the applied stress.

The deformation that occurs in the fluids can be extensional (elongational) or shear and is responsible for generating a flow characterized by the relative movement among the molecules of the material due to the action of an external force.

This deformation allows to obtain a parameter that can be seen as a determinant factor for the use and applications of fluids: viscosity. This property can provide information on structural variations that occur during the application of stress or even represent a direct measure of the quality of the fluid in service.

Viscous fluids can be classified as Newtonian or non-Newtonian depending on their rheological behavior involving viscosity with respect to time and shear rate.

In Newtonian fluids, the shear stress is proportional to the shear rate and the viscosity is the proportionality constant, that is, it does not vary with the increase of the shear rate. Due to the Brownian motion of the constituent molecules, the viscosity for almost all fluids, when in liquid state, tends to decrease as temperature increases, because the molecules tend to become less compact when warmed, and expand to occupy a larger volume leading to a decrease in the viscosity (Barnes et al., 1989). Regarding pressure, the viscosity tends to increase with it. (Junior, 2011). Some fluids such as air, water, saline, glycerin, oils and their derivatives are examples of Newtonian fluids.

With respect to non-Newtonian fluids they can be classified as time-dependent, time-independent or viscoelastic fluids.

For materials in which the viscosity varies with time at a constant shear rate they can be classified as thixotropic or reoptic fluids. Thixotropics are those that have their structure broken as the shearing time increases causing the viscosity to drop. This phenomenon is isothermal and reversible, because with the withdrawal of the shear stress, the fluid returns to its initial configuration, recovering its initial apparent viscosity. For these materials there is a time required for the viscosity to drop and then remain constant independent of the applied shear rate. However, the reoptics present an increase in viscosity with the increase of the shear time when subjected to constant deformation (Costa, 2017).

According to Bretas and D'Ávila (2000), for time-independent fluids, when there is no minimum stress required for the fluid to start flowing called the yield stress (τ_y), the viscosity may respond in three ways as the shear rate increases, or viscosity increases due to the disorder and approximation of the molecules, as is the case of the dilants or it remains constant as is the case of Newtonian fluids, or the viscosity falls as is the case of pseudoplastics. This drop in viscosity can be explained by three reasons:

- 1- When at rest, the particles are oriented at random and very close to each other. Upon being disturbed with increasing shear rate, these particles line up in the flow direction, reducing the resistance to this flow.
- 2- The fluid contains highly solvated molecules (ions of a dissolved substance combining with solvent molecules) and that with the shear rate, these molecules have the solvation layers destroyed.
- 3- In the case of some polymers in the molten state, when they are at rest, these have a highly tangled structure and with increasing shear rate, this structure is oriented in the direction of the flow assuming a linear form.

In the case of viscoplastic fluids having a yield stress, below which the material deforms in an unexpressive way, if the viscosity of the fluid after the breakage of the internal structure of the material remains constant, the fluid is classified as Bingham, otherwise, it is modeled by the Herschel-Bulkley equation (Costa, 2017).

The Herschel-Bulkley model describes fluids with an initial stress that causes a major change in material structure. This equation is given below:

$$\eta = \begin{cases} \frac{\tau_y}{\gamma} + K\gamma^{n-1}, & \text{se } \tau \geq \tau_y \\ \infty, & \text{se } \tau < \tau_y \end{cases}$$

Where τ_y is the yield stress, η is the viscosity, γ is the shear rate, K is the fluid consistency index and n is the Power-Law index, which if smaller than one characterizes a pseudoplastic fluid (shear thinning) and when larger than one characterizes a shear thickening fluid.

When the stress is below this yield stress, the fluid will have a viscosity tending to infinity, ie it will not flow.

Another model that describes the behavior of viscoplastic fluids is the so-called Bingham model. Its equation corresponds to the Herschel-Bulkley model when $n = 1$.

$$\eta = \begin{cases} \frac{\tau_y}{\gamma} + \mu_p, & \text{se } \tau \geq \tau_y \\ \infty, & \text{se } \tau < \tau_y \end{cases}$$

Where μ_p = plastic viscosity.

The flow pattern of a viscoplastic fluid is characterized by two distinct regions: undeformed regions, where stresses are less than the yield stress and deformation is extremely low, and deformed regions, which appear where stress level is greater than the yield stress. The classification of these zones allows to determine some important flow characteristics such as the pressure drop along the flow and the amount of fluid that can remain stagnant in a specific flow region. Therefore, studying the flow pattern and determining how it is affected by rheological and kinematic parameters is fundamentally important (Hermany, 2012).

Figure 2.1 illustrates the behavior of shear stress for time-independent and time-dependent fluids cited above.

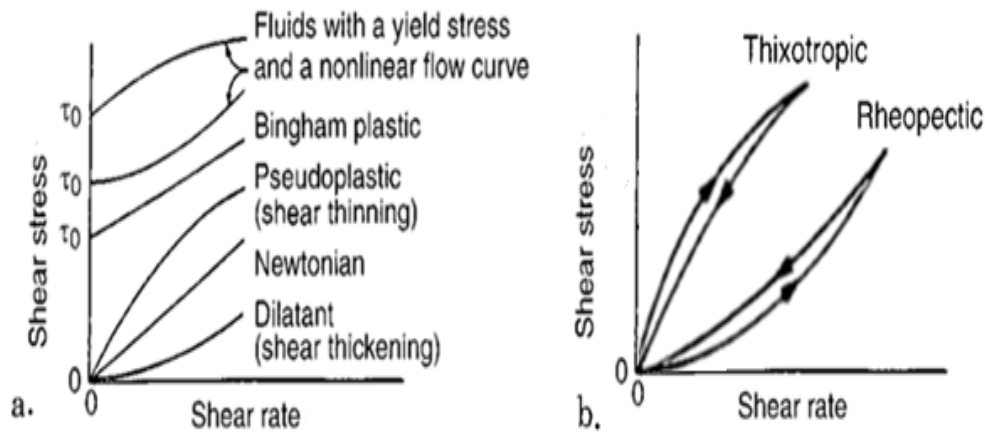


Figure 2.1 - Plots of shear stress versus shear rate for non-Newtonian and Newtonian fluids: **a.** time-independent **b.** time-dependent fluids. (Jaluria, 2001)

Another way of representing the rheological behavior of the independent fluids of the shear time is through the curve where the apparent viscosity is plotted as a function of the shear rate according to figure 2.2.

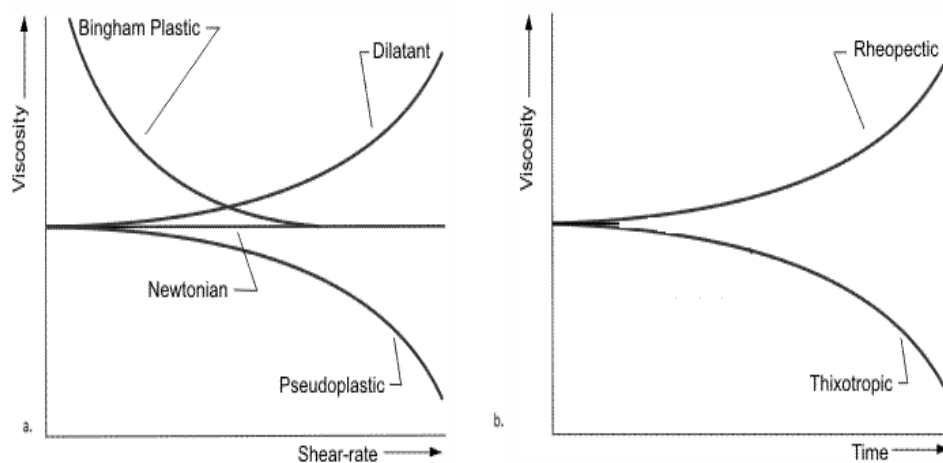


Figure 2.2 – Flow curve of: **a.** time-independent and **b.** time-dependent fluids (Richardson, 2011)

Viscoelasticity is a phenomenon that depends on time and only occurs in polymer systems. At the molecular level, when the entangled structure of the polymer undergoes the application of a constant stress, the molecules exert a

repressive response to this stress to maintain its more stable conformation. If this stress remains applied for a considerable time, the polymer chains begin to slide among them thereby deforming the entangled structure. By removing this stress, its molecules that are in a more elongated conformation tend to return to their initial configuration whose thermodynamic state is the most stable (Bretas and D'ávila, 2000).

The viscoelastic behavior of a polymeric materials can be divided into two regimens: non-linear or linear viscoelastic. In the non-linear viscoelasticity regime, larger deformations are applied, causing the molecules to leave their equilibrium condition, the structural level changes as the fluid deforms and the viscoelastic properties become dependent on the shear rate and the kinematics of the deformation.

In the linear viscoelastic regime, the polymer molecules are not removed from their equilibrium state because the deformations are small and slow, allowing the characterization of the material at a structural level. One of the most important tests in this regime is the small amplitude oscillatory shear (SAOS) that allows to evaluate the viscoelasticity of a material through two parameters: the storage modulus (G'), which gives the elastic measurement of the material, and the lost modulus (G''), which measures the capacity of the fluid to dissipate energy in form of heat.

These material functions and some other measures of rheological properties can be obtained through a rotational rheometer which measures the stress and deformation of the materials from a drag flow which can be imposed by a rotational (steady flow) or oscillating (oscillatory flow) movement of a geometry at an angular velocity. Figure 2.3 illustrates some geometries that can be coupled to the rheometer that are concentric cylinders (couette), cone-plate, parallel plates and double-gap and their choice depends on the range of viscosity and shear rate desired to obtain the measurements of the experiment, as well as the type of fluid.

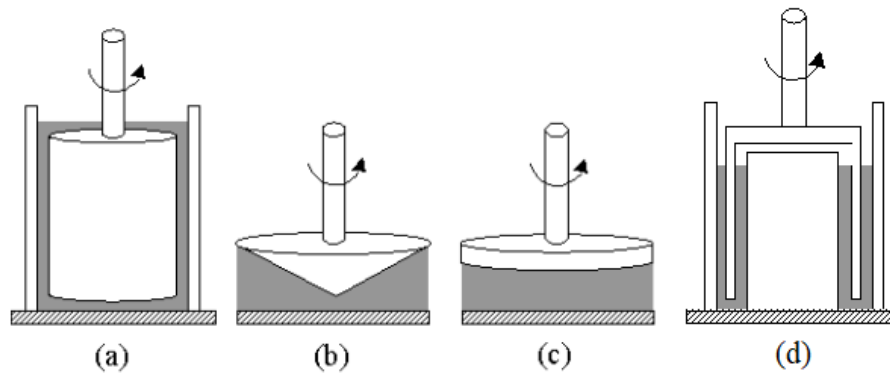


Figure 2.3 - Schematic diagram of basic tool geometries for the rotational rheometer: (a) concentric cylinders (couette), (b) cone-plate, (c) parallel plates and (d) double-gap.

The problem of wall slip that usually affects the reading of the rheometer in all types of geometry cited can be avoided by using grooved (highly roughened) surfaces.

In these types of geometries, a force is applied at the top of the rheometer producing a torque and causing that geometry to move giving speed to the fluid that is placed in the gap between the upper and lower parts of the geometry. This speed is controlled by an internal resistance, ie viscosity.

The rotational rheometer may be deformation or stress-controlled. In the case of deformation-controlled, a shear rate is imposed and the result stress is monitored, whereas in the stress-controlled rheometer a predefined stress is imposed and both the result stress and the deformation can be monitored.

To characterize the fluid rheologically some tests are done, for example: steady shear, flow curve, stress / strain sweep, frequency sweep.

The steady shear can inform the dependent or independent character of the time and indicate the time the sample takes to reach the steady state.

The flow curve allows the rheological classification of fluid behavior and an evaluation of the influence of several factors such as temperature, concentration, presence and size of suspended particles on the viscosity.

In the stress / strain sweep is possible to determine the linear viscoelasticity region, ie region with combination of viscous and elastic effects where the properties of the material are not influenced by the conditions of the test and the

material functions are independent of the applied deformation. With this test it is also possible to determine which modulus is superior in a specific region, whether it is storage (G') or lost (G''), thus verifying if there is a predominance of viscous or elastic effects.

The frequency sweep is done to obtain the characterization of the mechanical spectrum of the material, that is, the behavior of the storage (G') and lost modulus (G''), as well as the mean values of the phase angle ($\tan \delta = G'' / G'$).

The rheological tests mentioned above can be performed in three different types of shear flow: steady, oscillatory and transient. These shear flow differ in the way the deformation is applied to the sample. In the steady shear flow, continuous rotation is used to have a constant shear rate and thus measure the shear stress and the corresponding viscosity as a function of the shear rate, as in the case of the flow curve. This type of regime provides some important information about pseudoplastic and thixotropic behavior, as well as to determine the yield stress and enable to understand the behavior of these materials in real situations such as pumping, agitation and extrusion. Already in the oscillatory shear flow, the tests relate the angular velocity or imposed frequency with the resulting oscillatory strain or stress and are performed in a way that the samples are mechanically disturbed, but do not have their internal structures ruptured. In this shear flow, the tests of stress sweeps and frequency sweep are carried out. And, finally, in the transient shear flow, the deformation is fixed and the behavior of some properties is observed varying the time, as it is in the case of the test of steady shear.

LITERATURE REVIEW

This chapter begins by presenting basic concepts of nanotechnology science and the properties of nanofluids. Then, describes the characteristics and properties of some allotropes of carbon and its oxygenated derivatives and detailing the processing methods used to obtain graphene. After, it describes the properties of the polymer used in the present work. Finally, it highlights some results of works that followed this line of research.

3.1 NANOTECHONOLGY

Nanotechnology is an interdisciplinary field of research that studies the manipulation of matter at the atomic and molecular level. According to Valim (2015), nanotechnology can be defined as "the design, synthesis, characterization and application of materials, devices and systems that has a functional organization in at least one dimension on the nanoscale (approximately 1 to 100 nm)."

This science has as main objective the construction of new devices in nanoscale scales, through the atomic restructuring, potentializing the manufacture of these products and making them safer, durable, smaller and with greater performance when compared in larger scales. This higher performance of nanometric materials is due to the following reasons: increase in surface area, high surface energy, decrease in imperfections, and confinement of charge carriers in reduced nanoparticle dimensions (CAO, 2004). In this way, the researchers' focus is not on reaching individual control of the atoms but rather on creating structures that are more stable. Due to these peculiarities, this branch of science attracted the attention of several areas such as medicine, electronics, physics, chemistry, computer science, materials engineering.

According to Neto (2009), the American physicist Richard Feynman was the first scientist to conduct studies on nanotechnology and presented his project in

1959 in a lecture for the American Society of Physics. But only at the beginning of the 21st century did this science gain strength.

As previously mentioned, nanotechnology works with materials on a molecular scale and for this it is necessary to use high precision equipment such as scanning electron microscopy (SEM), scanning tunneling microscope (STM), among others, to understand the changes of the materials properties at the atomic level.

It is possible to observe several applications of nanotechnology in daily life, both in the textile field, with the production of fabrics more resistant to dirty and waterproof, and in electronics, with computers and mobile phones becoming smaller and faster.

In the pharmaceutical industry, polymer nanoparticles consisting of biodegradable polymers has been widely used in controlled drug delivery systems. The polymer used in the presente study, PEG 400, is one of the polymers used to this end. The nanostructures of such polymers act as transport compartments of active substances, and present some advantages when compared to liposomal systems, such as: good physical, chemical and biological stability, good reproducibility and, when applied to some substances, improve their chemical properties (Schaffazick, 2003).

Due to the diverse structures forms and spatial properties, interest and the quest for new knowledge about carbon nanostructures has been growing and gaining prominence (Aguiar et. al, 2015).

Nanotechnology also has disadvantages such as the possibility of generating nanopollutions caused by nanomaterials or during their manufacture. This type of pollution becomes more dangerous because the nanoparticles float easily through the air traveling over large distances and because human cells do not know nanopolluents, so they do not have "guns" to fight them, causing damage as yet unknown.

3.2 NANOFUIDS

Einstein (1956) defined nanofluids as two-phase suspensions with Brownian motion. However, in most applications, fluid is hypothetically considered to be only a single phase. Within the nanotechnology area, there was a growing interest in the nanofluid study because, through published works, it was possible to observe a significant improvement in some properties of the fluid base when placing small volumetric fractions of nanoparticles (Oliveira 2014). Nanofluids are designed by homogeneous suspension nanostructures with average sizes below 100 nm in conventional fluids.

The type of nanoparticle suspended in the mixture may be a factor in classifying nanofluids. Some materials such as ceramic oxides, metal oxides (CuO, ZnO, TiO₂, SiO₂), metals (Cu, Ag, Au, Fe), carbon nanotubes (single and multiple wall) and graphene are used for the production of nanofluids and are some of the different types of nanoparticles that exist. Figure 3.1 shows microscopic images of carbon nanotube nanofluids.

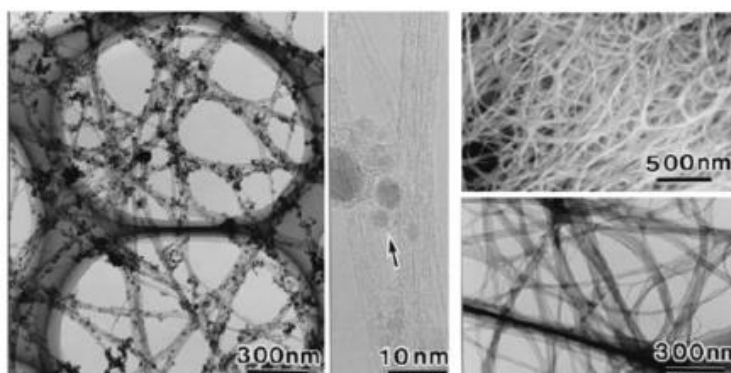


Figure 3.1 - Carbon Nanotube Nanofluids in 10nm, 300nm, and 500nm Distinct Scale Images (Hosokawa et al., 2007).

Nanoparticles can be produced by physical or chemical processes. Methods such as mechanical grinding and inert gas condensation techniques are considered physical methods whereas the techniques that use chemical precipitation, chemical exfoliation, chemical vapor deposition, microemulsions and plasma combination in gas phase methods are considered chemical processes. Figure 3.2 shows a scheme of the high pressure homogenizer for the production of nanofluids.

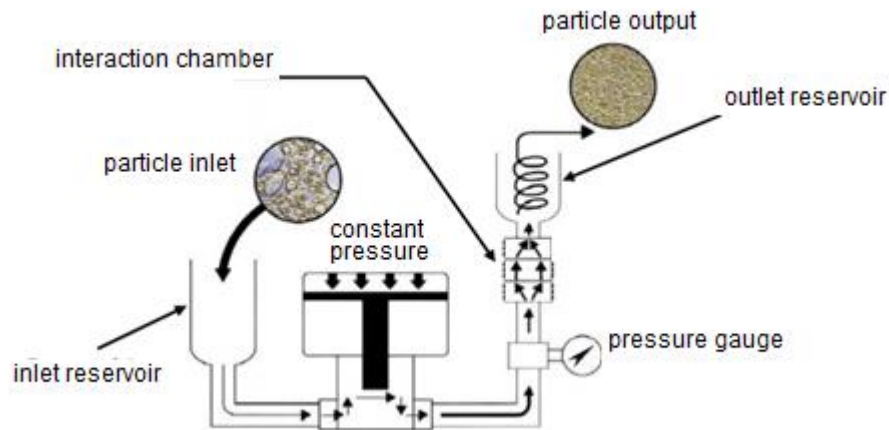


Figure 3.2 - Scheme of the high pressure homogenizer for the production of nanofluids (Hwang et al., 2008).

The homogenizer submits the particle at high pressure through a very narrow slit. After that, the fluids are accelerated over a very short distance at high speed. The high cavitation force breaks the particles, fragmenting them on a nanometer scale (Sousa, 2013).

There are two ways of preparing a nanofluid: either the nanoparticles are produced and dispersed simultaneously in the base fluid (one step) or first they are produced and then added to the base fluid (two steps). The first method avoids various processes such as drying, storage, handling and dispersion of particles thus obtaining a more stable nanofluid, but there is a preference for the second form of preparation. This preference is due to the ease of commercialization of these nanoparticles in powder form and because this process is an economic method for large-scale production, since nanostructure synthesis techniques are scaled up to mass production levels.

However, the two steps technique has some limitations regarding dispersion and solubility since these nanoparticles rapidly agglomerate and subsequently sediment after being dispersed in the base fluid because they are not capable of breaking the interactions that exist between the base fluid molecules (Oliveira, 2014). Figure 3.3 shows some common challenges of nanofluid development.

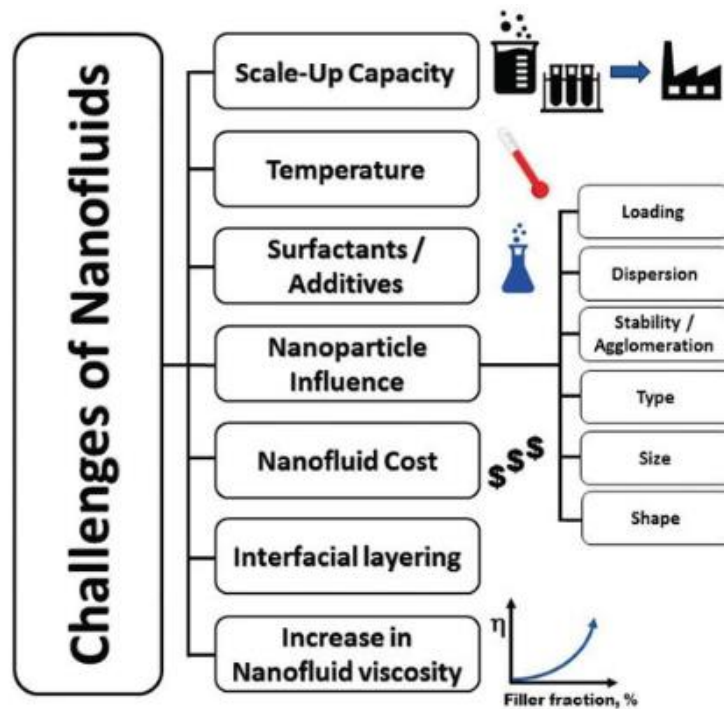


Figure 3.3 – Common challenges of nanofluid development
(Taha-Tijerina, 2018)

Although nanoparticles have unique properties, such as large surface area relative to volume and size dependent physical properties, which are capable of improving the properties of conventional fluids, the difficulty of achieving a stable dispersion has been a major challenge for researchers when there are no chemical changes such as pH change or surfactant addition. To solve this problem, homogenization of the dispersion is carried out by means of stirring techniques, such as the ultrasonic bath, magnetic stirrer and high pressure homogenizer. Factors such as intensity, particles sizes and time of stirring are also able to influence the effect of dispersion.

However, even after agitation, the Van der Waals forces are able to agglomerate these nanoparticles again resulting in the settlement as shown in figure 3.4 and to minimize this problem and to make those suspensions stable for a longer time, surfactants are added.

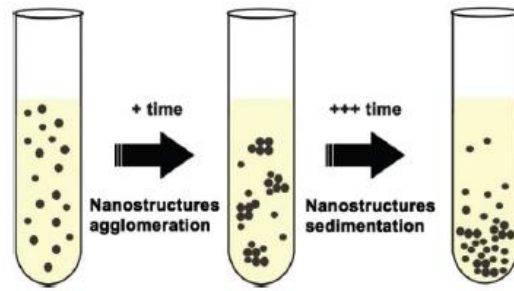


Figure 3.4 – Scheme of nanoparticles sedimentation over time
(Taha-Tijerina, 2018)

In addition to influencing stability, this agglomeration of the particles causes the effective surface area/volume to decrease, which affects the thermal conductivity performance of nanofluids, and because of these facts, questions about the factors that are capable of altering the thermo-physical properties should be studied through some methods of evaluation as a zeta potential (indicates the degree of repulsion between the particles and the stationary layer of liquid surrounding these particles), sedimentation rate, pH control.

Because the chemistry of the surface of nanofluids is complex there are differences in results among the studies carried out with regard to the characteristics of nanofluids and even so, the motivation to improve these characteristics and the study of possible future applications has grown.

Although standards and criteria for stability measurements have not yet been defined, the study of other properties such as thermal conductivity and viscosity are also required for the determination of possible applications.

The rheological behavior of nanofluids is an important issue. According to Mirmohammadi (2012), the addition of nanoparticles to a base fluid in addition to increasing thermal conductivity may change the rheological, thermal and mechanical properties of the fluid. Philip and Shima (2012) realized in their work that the results of the majority of experiments found in the literature about nanofluids do not follow the theories of classical continuum mechanics, since it is possible to observe an increase in viscosity, thermal conductivity and heat convection in nanofluids. The viscosity of nanofluids depends not only on the shape of the inserted nanoparticles, but also on the size and quantity. These nanoparticles form clusters which leads to increased viscosity.

Taha-Tijerina (2018) defined some parameters that are capable of affecting the viscosity of nanofluid such as preparation method, base fluid type, operating temperature, acidity (pH value), shear rate, use of additives or surfactants and particle aggregation. Some effects such as sedimentation, brownian motion and hydrodynamic diffusion can also affect the viscosity of these fluids.

Brownian motion, which is the random motion of particles as depicted in figure 3.5, tends to move particles from areas of higher concentration to areas of lower concentration. Aminfar and Motallebzadeh (2012) investigated the concentration distribution and velocity field of nanoparticles on water / Al_2O_3 nanofluid in a pipe and concluded that brownian forces have a greater impact on nanoparticle charge fraction distribution and velocity field when compared to other forces. The effects of Brownian motion only exist when the particles in the fluid are extremely small and are reduced as the particle size increases.

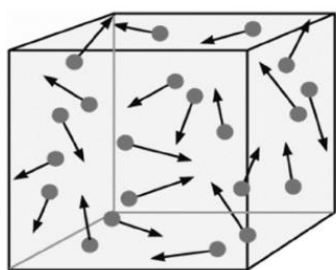


Figure 3.5 – Brownian motion of the particle (Das, 2017)

3.3 CARBON ALLOTROPES AND ITS OXYGENATED DERIVATIVES

Carbon, considered the basic structural element of organic chemistry and extremely abundant in the universe, has the ability to combine with itself and other chemical elements, creating numerous stable compounds. By performing three types of hybridization, it is capable of forming carbon chains with different configurations (distinct molecular and structural forms) and physical properties. Figure 3.6 shows some of the allotropic forms of carbon. Allotropic varieties can result from two situations: one refers to the amount of carbon atoms present in the molecules, the other to the form in which these atoms are arranged geometrically, ie their structural arrangement.

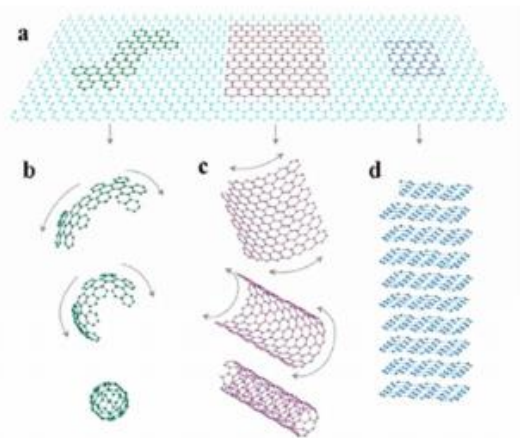


Figure 3.6 - Carbon Allotropes: a) 2-D graphene, b) Fullerene, c) Carbon nanotube d) 3-D grafite (Phiri et al., 2017)

Fullerenes and nanotubes can be visualized as a graphene layer wrapped in a spherical and cylindrical shape, respectively, and graphite as several graphene sheets arranged one above the other.

Table 3.1 shows some carbon allotopes and their respective physical and chemical properties. The differentiated bonds between the atoms themselves (both in number and in nature) are responsible for this diversity of properties.

	diamonds	fullerene	carbon nanotube	graphite
color	transparent	black	black	black to gray
density (g.cm ³)	3,515	1,69	1,33- 1,4	1,9 – 2,3
specific gravity	3,52	1,7 – 1,9	2	2,2
toughness	10	1-2	1-2	1-2
melting point (°C)	3550	>800	3652-3697	3652-3697
boiling point (°C)	4827	n/a	n/a	4200
Electric conductivity	insulating	semiconductor	cond/semi-cond.	conductor
hybridization	Sp ³ - tetrahedron	Sp ² - flat trigonl	Sp ² - flat trigonl	Sp ² - flat trigonl
crystal structure	cubic	truncated icosahedron	cylinder	laminar

Table 3.1 - Physical and Chemical Properties of Some Allotropic Forms of Carbon (adapted from Valim, 2015)

This bond between carbon atoms is formed by the hybridization process that occurs in some chemical elements and represents the union of incomplete atomic orbitals forming hybrids and increasing their stability. Hybridization depends on

the number of neighboring atoms that have space for an electron get into its orbital. Carbon hybridizations can be of three types: when it is possible to make bonds with 4 neighboring atoms, carbon assumes sp^3 hybridization, when it bonds to 3 neighboring atoms, the bond is of type sp^2 and when it bonds to only two neighboring atoms, carbon assumes sp hybridization. Figure 3.7 shows the carbon based nanomaterials and their hybridization states.

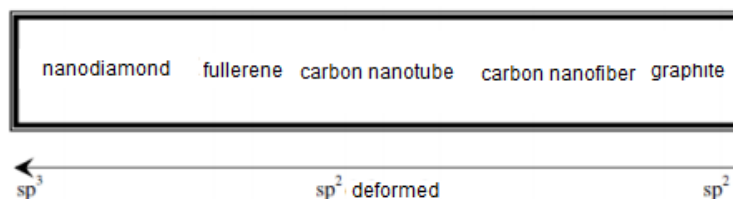


Figure 3.7 – Hybridization state of some carbon allotropes
(adapted from Negreti, 2016)

3.3.1 GRAPHITE

Graphite is a carbon allotrope formed by layers of sp^2 -hybridized atoms bonded together in hexagonal structure. Each layer that composes the graphite is a graphene sheet (Fim, 2012).

Graphite has some characteristics such as black color, a soft mineral and a great electrical conductor. Being a good conductor, it has applications in electronics such as electrodes and batteries. Graphite also has a high melting point, so it has applications as refractory material in steel casting crucibles and lubricating property due to its layered structure linked by weak van der Waals interactions, which gives it the character of a soft solid where its layers can slide over each other.

Although graphite is a common mineral of important industrial use (Russell, 1988) and of basic scientific interest (Jaszczak, 1995), it is rarely represented in mineral collections due to the rarity of good quality crystals (Sinkankas, 1964). Currently, this material has had a lot of industrial interest, because it is cheaper and more accessible way to get the graphene.

3.3.2 GRAPHITE OXIDE

Graphite oxide (GrO) is a composite of carbon, oxygen and hydrogen in varying proportions and one of the ways to obtain it is through chemical processes where graphite is treated with oxidizing agents. In 1859, Oxford Benjamin was the first chemist responsible for preparing graphite oxide by referring to this material in his works as “sheets of paper” with a thickness of 0.05mm (Brodie, 1859). However, only in 1975, a faster, more efficient and safer method has been developed that is used nowadays only undergoing some modifications, the so-called Hummers’ method. This method was proposed by scientists Hummers and Offeman where, in general, they oxidized graphite using a mixture of sulfuric acid, sodium nitrate and potassium permanganate (Marcano, 2010).

The oxidation degree and the synthesis method are the main parameters responsible for the different properties and structures of graphite oxide.

Although this material preserves the structural arrangement of graphite, it has a greater interplanar distance among its layers due to the insertion of oxygenated groups, as shown in figure 3.8.

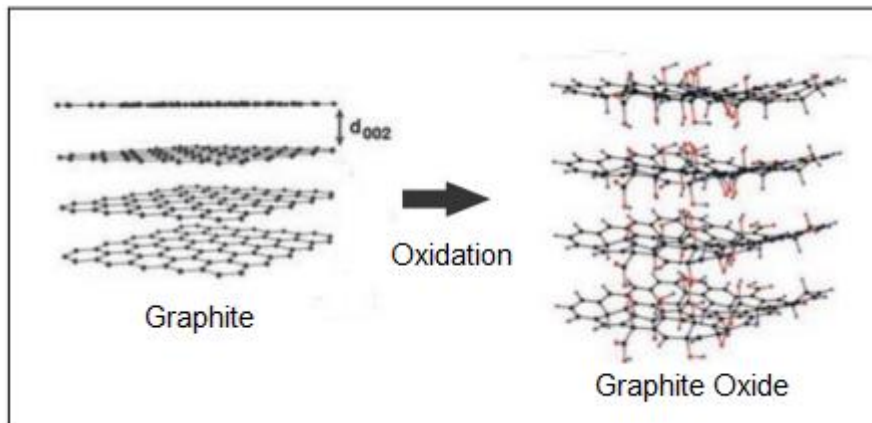


Figure 3.8 – Schematic representation of the graphite oxidation reaction (Sampaio, 2017)

Graphite oxide, being hydrophilic, can easily be dispersed in water and other polar solvents and when subjected to the sonication process, it is exfoliated to form GrO monolayers known as graphene oxide.

3.3.3 GRAPHENE

Graphene, seen in Figure 3.9, was first obtained and characterized in 2004. Two Russian researchers used the mechanical exfoliation technique when using an adhesive tape to peel a graphite plate and obtain fine graphene flakes. This discovery was a historic mark for science and awarded the University of Manchester, in 2010, the Nobel Premium in physics, broadening the view of scholars and expanding the study of different syntheses of graphene (Castro, 2011).

Like carbon nanotubes, the term graphene today corresponds to a family of compounds, from the monoatomic sheet to materials formed with ten neatly stacked graphene sheets. These materials, known as single-layer graphene, two-layer graphene, and multilayers graphene have distinct electronic properties due to the different electronic couplings among the various sheets in each of the structures. Although recently discovered and the newest member of the carbon allotropes family, graphene is already being considered, as well as carbon nanotubes, a highly strategic material (Oliveira, 2013).

Graphene is made up of a two-dimensional network of carbon atoms with sp^2 hybridized and has the same hexagonal arrangement as graphite, but consists of a single flat layer while graphite represents an aggregate of graphene sheets. This two-dimensional network obtained from graphite exfoliation has a high surface area.

Due to its excellent electronic, mechanical, thermal and optical properties, many studies about it being developed and its applicability have been increasing in several industrial sectors (Oliveira, 2015).

The sp^2 covalent bonds present in its structure are what provide flexibility and rigidity to the material, making it harder than diamond and if subjected to mechanical force, its plans bow (Geim and Kim, 2008) . Graphene also has excelente properties such as optical and electrical and thermal transport due to the delocalized electrons in the “p” plane that move around the structure (Castro, 2011).

Unlike GrO, graphene has a low defect density in its structure which leads to reduced dispersibility and a load mobility of up to $2000,000 \text{ cm}^2 / \text{V}$ at room temperature (Allen et al., 2009). These electronic properties of graphene make it widely used in electronic circuits, transistors and various high frequency equipment.

The thermal conductivity of graphene is superior to that of all known materials, even compared to copper, which is a material that conducts a lot of thermal energy. The conductivity of this sheet can reach 5000 W / m.K at room temperature and this information makes this material more exploited than carbon nanotubes when applied to thermal sensors and heat sinks (Balandin et al. Al., 2008).

Regarding to optical properties, graphene has a value of 2.3% optical absorbance, which does not allow its visualization with the naked eye, only in equipment capable of interacting with matter at molecular and atomic level. Optical absorbance is a property that measures the percentage capacity of materials to absorb radiation at a specific frequency when light passes through this material (Geim and Kim, 2008). This property combined with thermal conductivity and rigidity makes this material to be applied to solar cells, displays, transparent electrodes, among others (Castro, 2011).

According to Lacerda (2015), in addition to these applications previously mentioned, graphene can be applied in several other industry segments:

- Being extremely light, graphene-based compounds have been used in the aeronautics industry.
- At room temperature, the travel speed of electrons in graphene is higher than in other materials, which increases the speed of wireless communication and enables the manufacture of computers and mobile phones more powerful.
- Because it is transparent, graphene can be used in monitors, giving them greater brightness and contrast.
- By increasing the hardness of the materials on which it is deployed, graphene makes bulletproof vests lighter and stronger than today's.

Although this material has excellent properties and numerous applications, the main challenge for scientists is to obtain large quantities of this material with the lowest cost and highest structural quality (high purity) possible, which has led to the emergence of various synthesis processes.

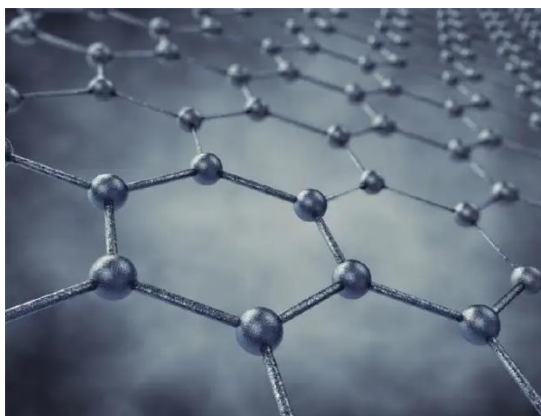


Figure 3.9- Graphene hexagonal crystal structure representation
(hypescience, 2014)

3.3.4 METHODS OF OBTAINING GRAPHENE

Although this material has excellent properties and numerous applications, the main challenge for scientists is to obtain large quantities of this material with the lowest cost and highest structural quality (high purity) possible, which has led to the emergence of various synthesis processes.

In the science world, studies are being conducted to obtain graphene more simply and at lower cost. A negative aspect of obtaining this material is that its ideal properties are available only when isolated, ie if the synthesized graphene remains attached to another material, these properties are reduced. Currently, there are two process routes: 1) bottom-up, which is related to material synthesis, and 2) top-down, which consists of material fragmentation to the desired scale (Fim, 2012). The generic scheme of both methods is represented in figure 3.10.

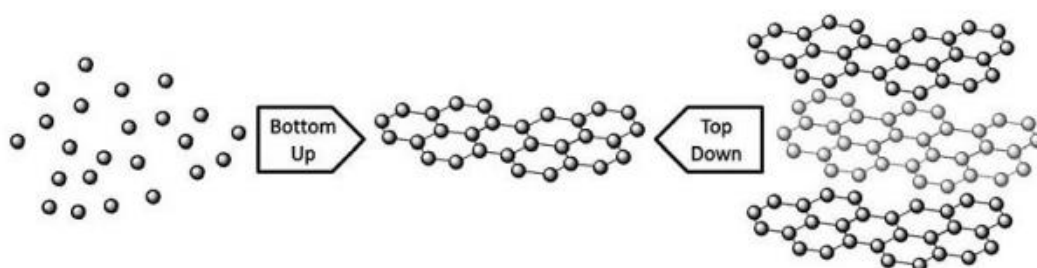


Figure 3.10 - Graphene production scheme by bottom-up and top-down
(Maraschin, 2016)

Bottom-up processes synthesize graphene from simple carbon atoms such as methanol and ethanol, with a lower degree of defects (a crucial factor for electronic applications). However, they are not applications in nanofluids, as require large quantities of this material. Table 3.2 presents some of the routes of this process and their respective characteristics:

method	thickness	length	advantage	disadvantage
chemical vapor deposition (CVD)	few layers	centimeter (cm)	large length, high quality	low production
bow discard	monolayer, bilayer, few layers	between 100nm and some μm	$\sim 10\text{g} / \text{h}$ production	carbonaceous impurities
epitaxial growth in SiC	few layers	up to cm	large area of pure graphene	low production
NTC decompression	multiple layers	some μm	size controlled according to the starting NTC	expensive raw material, oxidized graphene
CO reduction	multiple layers	up to μm	leaves without oxidation	alpha-Al ₂ O ₃ contamination

Table 3.2 - Bottom-Up Processes for Graphene Synthesis (Negreti, 2016)

The top-down processes shown in Figure 3.11 consist of separating the stacked layers of graphite by mechanical or chemical exfoliation producing individual graphene sheets. These processes when compared to bottom-up processes are evaluated as best for their low cost and high yield. However, these methods still need to be improved by increasing their reproducibility and large-scale production with process control (Maraschin, 2016).

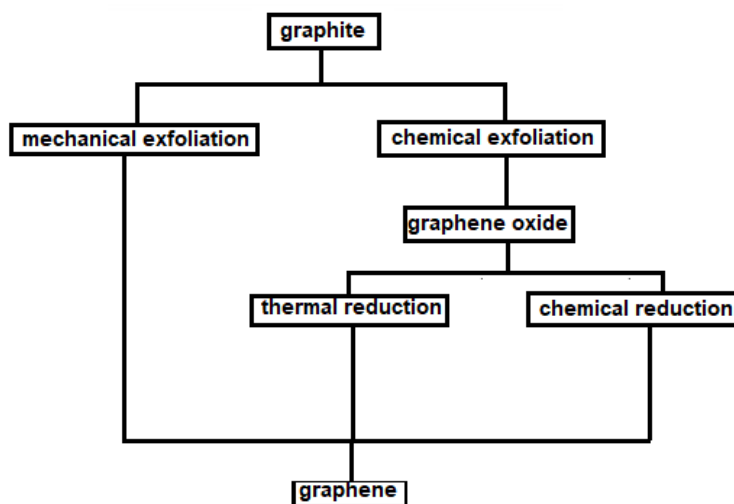


Figure 3.11 - Top-down Process Schemes

(adapted from Camargos e Silva, 2017)

Mechanical exfoliation is the precursor method of graphene isolation in which the van der Waals forces among the graphite layers are broken using an adhesive tape producing samples with excellent structural quality (perfect crystallinity) but with low yield, making the process not feasible for practical applications. At the research level, this process is the most suitable for the production of graphene (Junior and Lobato, 2017).

Chemical exfoliation is based on the oxidation of graphite with the addition of oxygenated groups increasing the interplanar distance among the layers and turning the sp^2 carbons of the lamellae into sp^3 forming the GrO. These oxygenated portions give the material a hydrophilic character making it easier to disperse in water. Using an ultrasound bath, the GrO's three-dimensional structure crumbles into individual GO sheets. And finally, GO is transformed into reduced graphene oxide (rGO) through thermal reduction through high heating rates or chemical reduction, made by reducing agents such as hydrazine and sodium borohydride. Through chemical reduction it is possible to restore the π network and the electrical conductivity of the material, making the reduced graphene oxide similar to graphene (Camargos e Silva, 2017).

According to Negreti (2016), Because chemical exfoliation has many variables involved, the end products have very different properties and characteristics, which makes it difficult to compare produced samples compromising factors such as reproducibility. This process has a low cost and high yield when compared to other

processes, but the presence of oxygenated groups in the basal plane of GO sheets generates samples with low structural quality. Among the different chemical exfoliation routes, the proposals by Brodie, Staudenmaier and Hummers and Offeman stand out.

In 1859, Brodie synthesized GO by adding potassium chloride and graphite to the steaming nitric acid to form a material composed of carbon, oxygen and hydrogen.

In 1898, Staudenmaier refined Brodie's technique by adding salt in various aliquots throughout the reaction and sulfuric acid to obtain a more oxidized GO (Negreti, 2016).

Finally, Hummers and Offeman developed a reaction composed of concentrated sulfuric acid and potassium permanganate generating a higher oxidation end product and not releasing toxic and explosive gases such as ClO_2 produced by Staudenmaier's method (Valim, 2015).

In order to accelerate the process of obtaining GO while at the same time becoming more oxidized and less toxic, the Hummers method has been modified over the years. This work used the modified Hummers method, but with the intention of avoiding the production of nitrous gases did not have the addition of sodium nitrate and potassium permanganate was added in portions to better control the temperature, as opposed to Hummers made by adding in a single serving

3.3.5 GRAPHENE OXIDE

Graphene oxide is a nanomaterial derived from graphite oxidation through chemical methods such as the Hummers method, maintaining the same structural arrangement constituting a hexagonal carbon network. The main differences between these materials are that GO microscopically is composed of only one layer, while graphite presents several layers in its structure and, as a consequence of oxidation, presents in its constitution functional groups such as carboxyl, hydroxyl and epoxy (Horszczaruk et. al, 2015). The synthetic process of GO mainly contains two steps: oxidation of graphite and exfoliation of graphite oxide, as shown in Figure 3.12.

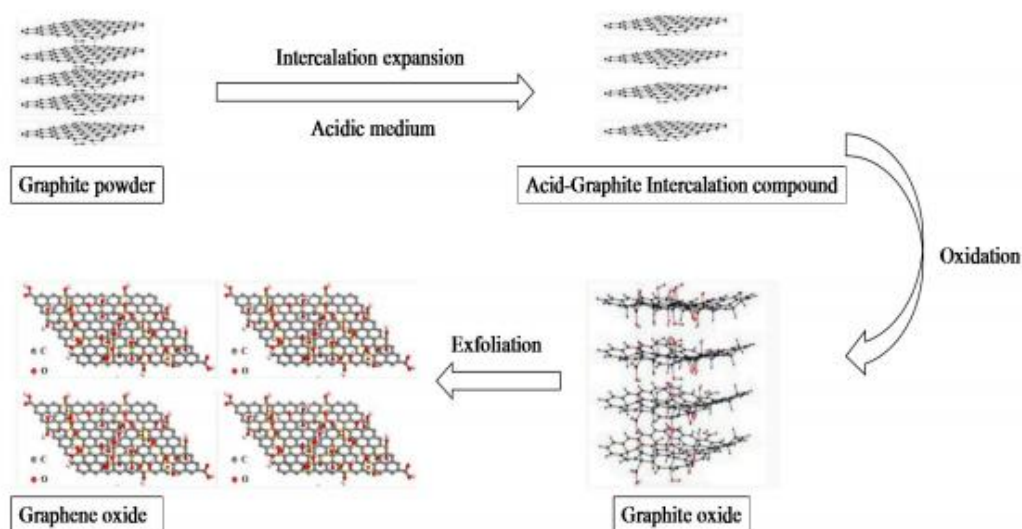


Figure 3.12 – Schematic illustration of GO preparation process
(Ma, 2017)

Since their discovery, scientists have been describing different models for the structural arrangement of graphene oxide. The oldest theory is that of Hofmann and Host who said that the structure of the GO consisted of epoxy groups in the baseline plane of graphene. Later, Ruess discovered that there was also the presence of hydroxyl groups in its structure as well as noticing that there were sp^3 -like bonds in the plane. In addition to these, some other models have also been proposed, however, the most accepted is the Lerf and Klinowski model. Figure 3.13 shows some of the main structures proposed for graphene oxide (Dreyer et al., 2010).

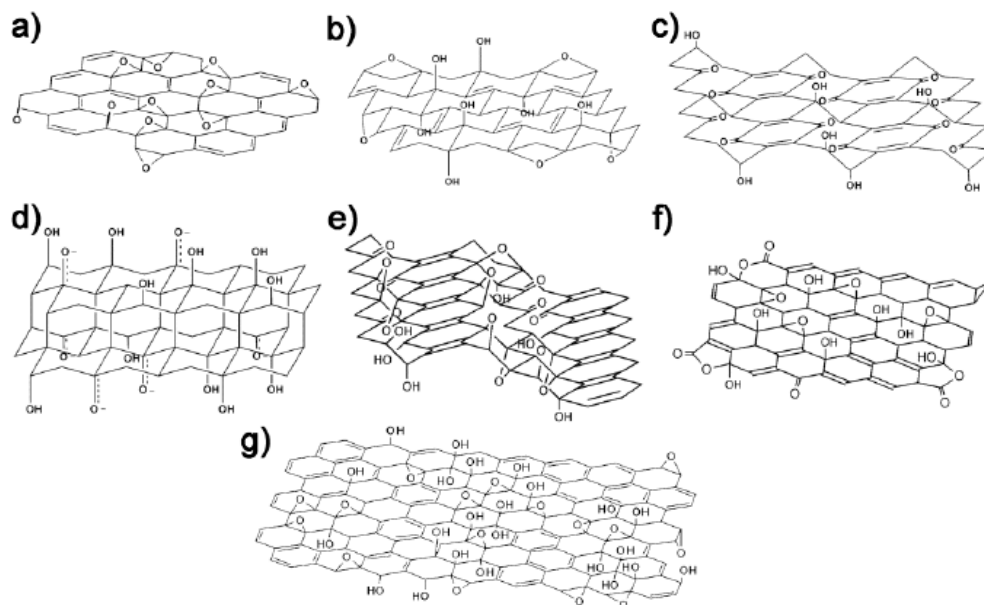


Figure 3.13 - Examples of models presented for the graphene oxide structure proposed by: a) Hofmann b) Ruess c) Sholz e Boehm d) Nakajima e Matsuo e) Dékany f) Ajayan g) Lerf e Klinowski (Cardoso, 2015)

According to Dimiev (2017), based on its two-dimensional geometry, graphene oxide can be seen as an excellent material to be incorporated into polymeric matrices improving properties, as it consists of a sp^3 hybridizing carbon atoms flat sheet due to the insertion of oxygen atoms in its structure. This insertion of oxygen atoms generates defects in the structure of graphite converting it from electrical conductor to insulator. Also, in addition to giving it the hydrophilicity property, that is, the ability to disperse and form stable colloidal solutions in water and some low molecular weight alcohols, it provides an adjustable bandgap opening which is responsible for optical and exclusive electronic properties.

The GO has a high specific surface that can lead to increased surface hardness of the material, since the pores in the composition of some materials such as lime paste can be filled by small particles of GO making the material more solid and compact.

One of the main problems related to humanity's survival is water contamination. Failure to treat waste combined with improper disposal of emerging contaminants can lead to irreversible damage to the environment and consequently to humans (Sui et al., 2011). A technique used for water treatment that has been widely

implemented in recent years because it is considered cheap, efficient and easy to implement is made by the adsorption process (Kemp, 2013). Graphene oxide, when compared to other materials, stands out for presenting interesting texture properties and great chemical stability, which makes this nanomaterial an adsorbent potential for the removal of contaminants in water (Avila, 2017).

In addition to these applications, GO can be applied in some other areas such as computing, health, energy as it is a very versatile material. In computing, this new nanotechnology, when implemented in RAM memory, makes it denser, faster and more energy efficient. In health, GO can be used as a biosensor and antibacterial. And in terms of energy, new more efficient batteries are being made by implementing graphene oxide in these materials (Cardoso, 2015).

Finally, GO can be used as an intermediate to obtain GrO (reduced graphene oxide) which is similar to graphene but with some defects. And as the process for obtaining large-scale graphene is having difficulty, the use of GO and GrO has become an affordable process. Reduced graphene oxide is also known as chemically modified graphene and what distinguishes it from graphene is that it contains defects in its structure, residual oxygen and other heteroatoms, as shown in figure 3.14.

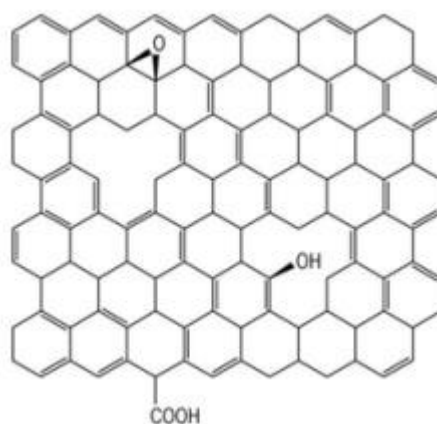


Figure 3.14 - Schematic structure of reduced graphene oxide
(Griggs and Medina, 2016)

3.4 POLY(ETHYLENE GLYCOL)

The PEG nomenclature is intended for compounds of low molar mass (below 20,000 g / mol) and the designation PEO, poly (ethylene oxide), is restricted to compounds of high molar mass (greater than 20,000 g / mol). PEGs having molar masses less than 1,000 g / mol are provided in the form of stable colorless solutions or viscous liquid. Those of high molar masses, above 1,000 g / mol, are found in the form of powder, waxy type solids. Therefore, it is possible to observe that the consistency increases as the molecular weight increases (Ribeiro, 2001).

Some characteristics such as the molecular mass distribution, the presence of branched chains and the molecular mass affect the rheological behavior of any polymer (Vasquez, 2007).

PEGs are obtained from the polymerization reaction of polyethylene oxide. In each unit of these oxides there are active sites (oxygen with free electrons) responsible for the interaction with the water molecules (Santos, 2011). In figure 3.15 it is possible to observe the partial planar representation of a PEG molecule.

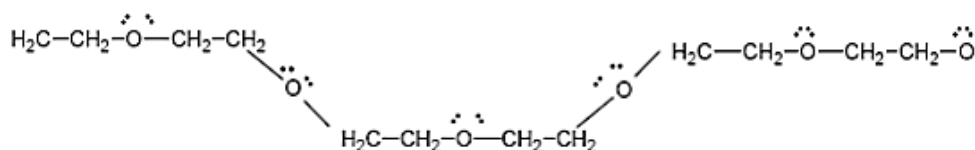


Figure 3.15 – Partial planar representation of the PEG molecule with the available sites for interactions with the other components of the system (Santos, 2011).

These polymers are generally non-toxic, biocompatible, hydrophilic, soluble in organic solvents, and have good thermal stability, low volatility and are considered non-ionic products (Abd Alla, 2004). As for the rheology of these compounds, they are Newtonian and it is possible to observe an increase of the viscosity with the increase of its molecular mass.

PEGs are pharmacologically inactive substances, i.e., constitute a group of excipients, are employed as bases for ointments, plasticizers, solvents and also as lubricants of capsules and tablets by completing the specified mass or volume by aiding in the preparation or stability of the product and by adjusting its consistency.

The excellent biological compatibility of the polymer and its chemistry has improved the development of hydrogels for applications in regenerative medicine (Nagarajan, 1998).

Another important property of this macromero is hygroscopy, that is, its ability to absorb air humidity. This property becomes even stronger with the decrease in molecular weight of the polymer. Due to this and its low cost, there has been an expansion in its use in biomedical, chemical and industrial applications (Oshima, 2008).

Several sectors such as cosmetic, dental, pharmaceutical, among others, have used PEG due to its excellent chemical properties and because it is considered a bioactive molecule, that is, it has several effects on living organisms and may be associated to changes in its behavior, physiology or metabolism. In addition, PEG was considered a non-antigenic or immunogenic molecule, causing the Food and Drug Administration (FDA) to approve its internal consumption, allowing its use in cosmetics, soaps and medicines (Pereira, 2008).

PEGs for having activity on surface tension are also considered excellent emulsifiers of oil and water being used as surfactants.

3.5 PREVIOUS WORKS

Naficy et al. (2014) studied the viscoelastic behavior of GO dispersions in water and concluded that at extremely low concentrations, GO sheets are randomly dispersed in the solution. As concentration increases, some nematic orders begin to appear. In this region, the storage modulus (G') increases and exceeds the loss modulus (G''), while the loss modulus remains almost constant with frequency. This can be attributed to the increase in the volumetric fraction of colloidal particles that gives the system elasticity. An additional increase in concentration results in greater packaging of the nematic phase. Upon reaching critical concentration, as the formation of the nematic LC phase is completed, an additional increase in volume fraction results in the simultaneous increase of both modulus, with the storage modulus increasing much faster than the loss modulus.

Shu et. al (2015) investigated the effects of graphene oxide concentrations in pure water and subsequently the effects of PEG (with molecular weight of 20,000 g/mol) concentration on the rheological behavior of GO/PEG aqueous dispersion

through steady state shear. They concluded that aqueous GO dispersions changed the behavior of Newtonian fluid to pseudoplastic with increasing GO concentration (c_g) and that the critical concentration of isotropic-nematic phase transition to aqueous GO dispersions was approximate 6mg / mL. Analysing the tests on non-linear flow to evaluate the effects of PEG concentration in GO/PEG aqueous dispersions, they concluded that for all concentrations tested in this study, the viscosity of dispersions decreases with increasing shear rate and as long as the PEG concentration (c_p) increases, the viscosity value firstly decreases, then increases again.

Giudice and Shen (2017) analyzed the rheological characterization of graphene oxide aqueous dispersions through measurements in oscillatory linear shear flow, steady shear flow and transient shear flow. Aqueous dispersions of GO of different concentrations (ϕ) were prepared and analyzed. First, they concluded the critical concentration (ϕ_c) exists, below which G-O sheets are dispersed, and above which they self-organize. Secondly, in tests conducted in linear oscillatory shear flow for dispersions below the critical concentration (ϕ_c), they concluded that the viscous response prevailed over the elastic response due to the drag of the GO sheets. And for dispersions with concentration above critical concentration, elastic response due to the G-O self-aggregation prevails over the viscous response due to the drag of the clusters. To analyze the responses obtained in the steady-state and transient tests, the Peclet number that determines whether the dominant mechanism is brownian diffusion or convective flow was evaluated. In steady-state tests, at $\phi/\phi_c > 1$, and at low Pe, G-O sheets self-aggregate, while at high Pe such aggregates disassociate. And finally, in transient shear flow, they concluded that G-O aggregates are reversibly formed once the flow is arrested; thus G-O dispersions act as thixotropic fluids.

Nanotechnology works with structures of the order of magnitude of the nanometer, that is, 10^{-9}m . These structures are so small that they are not visible to human eyes, or possible to be touched. For this reason, in order to collect information about these structures it is necessary to use equipment capable of interacting with matter at the molecular and atomic level. The characterization of these nanoparticles very important for the analysis of physical and chemical properties of a polymeric nanofluid.

4.1 X-RAY DIFFRACTION (XRD)

The diffraction is a phenomenon characteristic of the wave motion and is observed when a wave is "deformed" by an obstacle that has dimensions comparable to its wavelength. In the case of X-rays whose wavelength is of the order of Angstroms (10^{-10}m), they will only undergo diffraction when they focus atomic-level structures (Santana, 2006).

X-ray diffraction is a non-destructive technique, which is mainly used to characterize crystalline materials. It basically consists of the electromagnetic radiation bombardment in a certain sample that is positioned between the source and the detector, promoting a scattering of this beam, thus allowing the study of the effects caused by the material on the diffraction beam and characterizing the crystalline structure of that material. The atoms in the Crystal behave as scattering centers of X-rays. Figure 4.1 presents the experimental tool used for the application of this technique.



Figure 4.1 – Experimental tool used for the application of the X-Ray Diffraction technique (XRD)

4.2 RAMAN SPECTROSCOPY

Raman scattering spectroscopy is used to characterize carbon and its allotropes, differentiating crystalline from amorphous structures. The objectives of this tool are to investigate the vibrational spectra, the electronic structure and to identify the type of primary bond that is occurring between the carbons present in this structure. It is also possible in this technique to verify if the graphite oxidation process occurred as expected.

This technique consists in the incidence of a monochromatic beam on the surface of a material causing its absorption and scattering. Raman scattering is a phenomenon that can be observed when a small portion of the scattered light presents energy different from the incident light, although the light that spreads can present energy equal to the incident. Because it is a non-destructive method, this technique is quite applicable in the analysis of carbonaceous materials, mainly because it is able to differentiate the various carbon structures. Figure 4.2 illustrates the equipment used for the use of this technique.

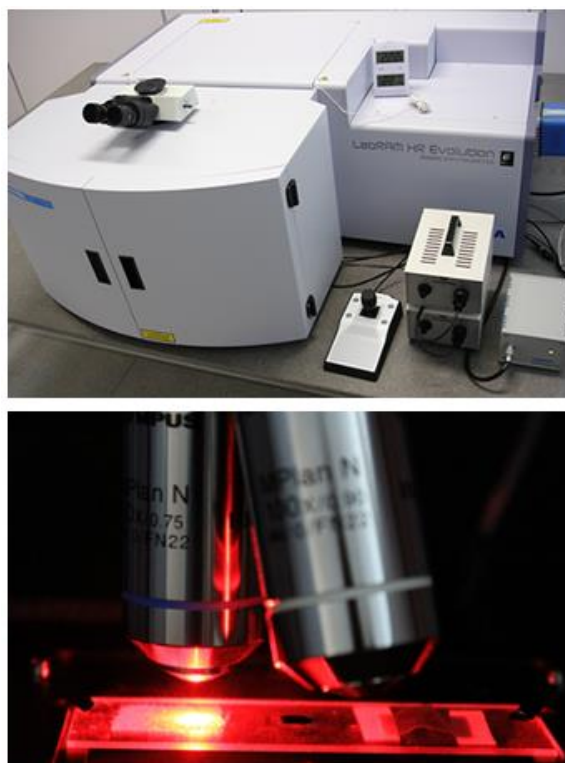


Figure 4.2 – Raman spectrometer (IMC Laboratory of Raman spectroscopy of the University of Caxias do Sul)

4.3 THERMOGRAVIMETRIC ANALYSIS (TGA)

It is a thermoanalytical technique that allows evaluating the thermal behavior of materials and uses a thermobalance where the sample is placed for analysis. This sample is heated and during its heating it is possible to monitor the loss or mass gain of the sample as a function of time or temperature under controlled atmosphere conditions. Figure 4.3 illustrates the apparatus used to perform this technique.



Figura 4.3 – Apparatus used to perform TGA

Figure 4.4 shows the thermogravimetric curve of graphite with different sizes. It is possible to observe the beginning of the mass loss of graphite crystals around 750-800°C proving that the graphite is thermally stable due to its high structural stability.

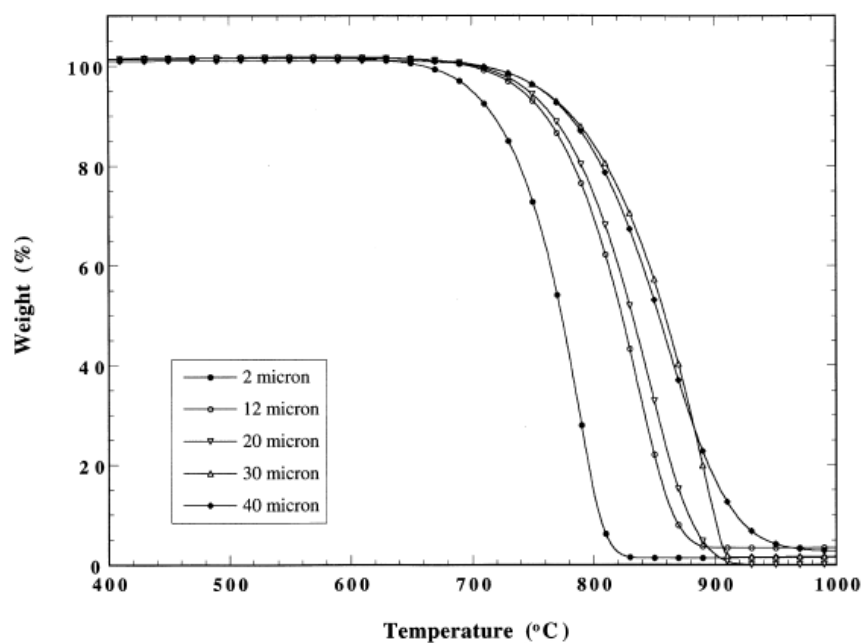


Figure 4.4 – TGA measurement of the oxidation of natural graphite in air.
Heating rate 10°C/min (Jiang et al., 2000)

4.4 ATOMIC FORCE MICROSCOPY (AFM)

This technique, which allows precise measurements on nanoscale, uses a microscope containing a probe with a tip that sweeps the surface of the sample and also analyzes changes in its relief (changes resulting from the interaction between the atoms of the tip of the AFM and the atoms of the sample surface). It also maps some mechanical properties and provides an overall aspect of the distribution of sample leaves. This microscope also provides images of the surface of certain material allowing the study of its morphology. Figure 4.5 shows the microscope used for the characterization by AFM.

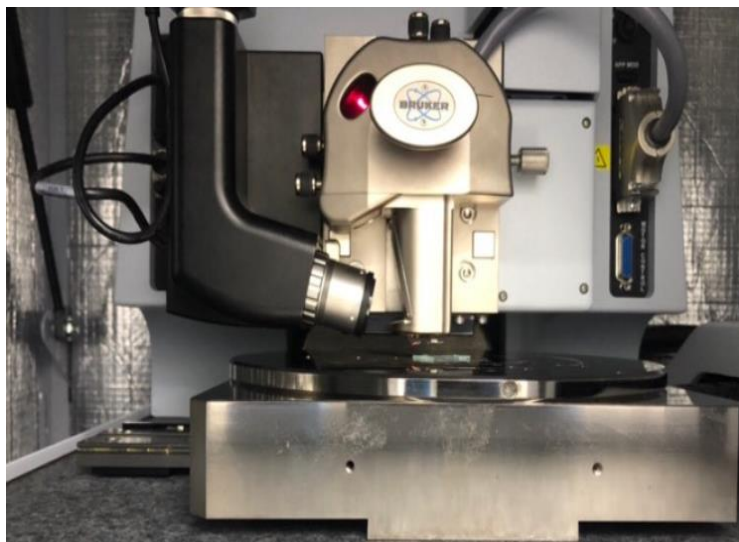


Figura 4.5 – microscope used for the characterization by AFM

The operating principle of AFM is based on the interaction that occurs, along the scan, between the atoms that make up its tip and the atoms that compose the surface of the sample (García and Pérez, 2002). As the tip of the probe is approached with the sample, this tip is drawn by Van der Waals forces. As it approaches, repulsive forces are generated by the fact that their electronic clouds begin to repel (at a blond distance), weakening the attractive force. These rod movements that reflect the shape of the surface are monitored by a laser beam.

4.5 INFRARED VIBRATIONAL SPECTROSCOPY (FTIR)

This technique is based on absorption spectroscopy that identifies a compound through the infrared region, and investigates the composition of a sample or provides evidence of the presence of functional groups. To obtain the measurements of a sample, the amount of energy transmitted by a beam of infrared radiation passing through the sample is recorded. A molecule passes into a state of excited energy when it absorbs radiation and this absorption occurs when the radiation has the same frequency as the vibration of the bond, thus increasing the amplitude of the vibration. The frequency or wavelength of absorption will depend on the relative masses of atoms, bond strengths and the structural arrangement of atoms in the compound. Figure 4.6 illustrates the equipment capable of performing this characterization technique and figure 4.7 shows the graphite FTIR spectrum.



Figure 4.6 – FTIR Spectrometer ([ltsscientific.com/product/vertex-7070v-ftir-research-spectrometers/](https://www.ltsscientific.com/product/vertex-7070v-ftir-research-spectrometers/))

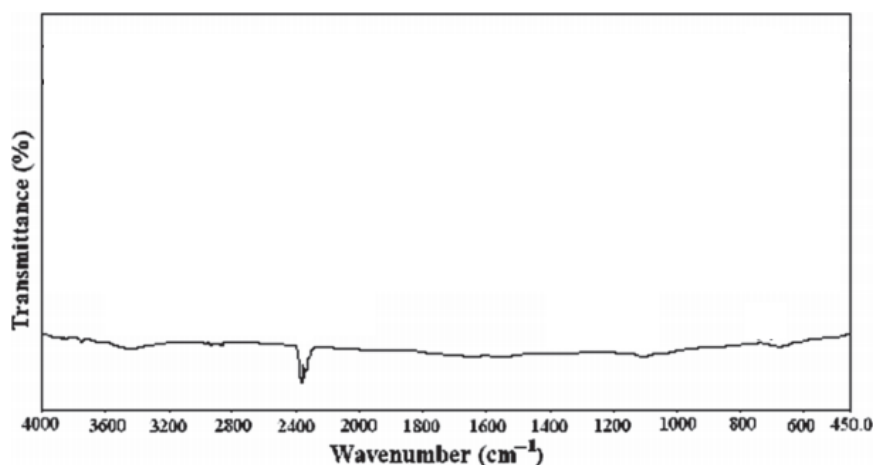


Figure 4.7 – Graphite FTIR spectrum (Kartick, 2013)

MATERIALS AND METHODS

This chapter presents the materials and methodologies used for the synthesis of GO and the suspension of GO in PEG. It also describes the rheological tests performed and the characterization methods employed.

5.1 MATERIALS

Table 5.1 show all products and reagents used, such as the supplier company for the graphene oxide production:

Products/reagents	Supplier company
Graphite powder <45 μ m, \geq 99.99% trace metal basis	Sigma-Aldrich
H ₂ SO ₄ (99%)	Sigma-Aldrich
KMnO ₄	Sigma-Aldrich
Poly(ethylene glycol) M _w 400g/mol	Sigma-Aldrich
C ₂ H ₅ OH	Synth
HCl (ACS reagent, 37%)	Synth
H ₂ O ₂ (30% m/m)	Synth
Deionized water	PUC

Table 5.1 – Products, reagents and the supplier company for the graphene oxide production.

In addition to these materials, some laboratory equipment such as volumetric flask, beakers and funnel were used to obtain GO through the Modified Hummers method. Figure 5.1 shows some of these equipments.



Figure 5.1 - Some laboratory equipment were used to obtain GO through the modified hummers method

5.2 SAMPLE PREPARATION METHOD

Graphite oxide was obtained by modified Hummers method and used in samples preparation of different concentrations. This method consists in the addition of 1g of graphite and 60mL of sulfuric acid (H_2SO_4) in a 500mL round bottom flask. According to figure 5.2, this reaction is performed under low temperature (emerged in an ice bath) and under agitation at a frequency of 500 Hz (a medium goldfish is placed inside the flask and through a magnetic stirrer provides such agitation) for 15 minutes. Thereafter, 3.5mg of potassium permanganate (KMnO_4) is added slowly for 15 minutes. It is important to mention that the addition of permanganate must be done slowly due to the fact that an extremely exothermic reaction occurs and with a very high kinetic velocity. These reagents are added with the intention of expanding the structure and oxidizing the surface of the graphite sheet due to the presence of oxygenated functional groups. At the end, the system was removed from the ice bath and allowed to stir under the desired oxidation time. For this work the oxidation times used were 2h and 96h.

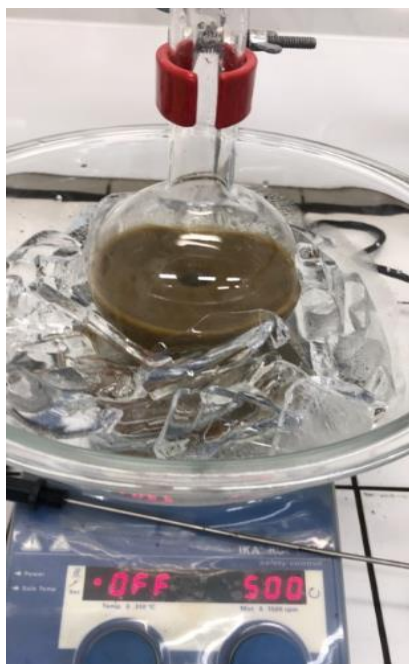


Figure 5.2 – Reaction among graphite, sulfuric acid and potassium permanganate under low temperature and agitation

After the oxidation step, the system returned to the ice bath and 200mL of deionized water was slowly added to stop the reaction. At the end of the dilution, a portion of aqueous solution of hydrogen peroxide (H_2O_2) was added until it stopped bubbling because the reagent neutralized the ions presents in the solution. At the end of the synthesis, the flask was removed from the ice bath and allowed to stand for 12 hours to allow the decantation to occur.

After that time, the supernatant was discarded and the generated product was filtered with a vacuum pump to speed up the filtration process and washed in the following order: 500 mL of deionized water, 250 mL of a 10% aqueous hydrochloric acid solution, 500 mL of ethanol and finally 250mL of deionized water again. The deionized water was responsible for the elimination of the salts, the hydrochloric acid for the removal of the metal ions and the ethanol for the removal of the organic residues. To obtain the GO with 2 hours of oxidation, the washing process took on average one day, while for obtaining the GO with 96 hours of oxidation, this process took an average of 3 weeks. Figure 5.3 illustrates the generated product being filtred with a vacuum pump.



Figure 5.3 - The generated product being filtered with a vacuum pump.

The obtained product was placed in the oven at 60°C to dry for a period of 12 hours. After being removed from the greenhouse, the material was macerated and dispersed in the polyethylene glycol with the intention of preparing suspensions with concentrations: 0.1, 1, 10, 20, 40 and 80mg / mL. These colloidal suspensions of graphite oxide were exfoliated in an ultrasonic bath at 40°C for a period of 4 hours, and then due to the exfoliation, graphene oxide (GO) was obtained. Figure 5.4 shows the product being macerated and figure 5.5 shows the colloidal suspensions being exfoliated in an ultrasonic bath.



Figure 5.4 – The final product being macerated



Figure 5.5 - The colloidal suspensions being exfoliated in an ultrasonic bath.

5.3 CHARACTERIZATION

The Raman spectrum of graphene oxide were obtained by the Witec Alpha 300R Raman Spectrometer. The equipment was calibrated using a silicon wafer (Si), with a grating refraction index of 600 g/mm (grades per millimeters), integration time of 0.25 seconds, 50x objective lens and 532nm laser. The sample was prepared from the dilution of 1 mg GO in 1mL of deionized H₂O, dropping one drop of the solution onto silicon oxide substrate.

In order to determine, by AFM, the sheets dimensions and thickness of the GO flakes obtained, the Bruker Model Icon Dimension Microscope with probe with tip covered with Si was used. A resolution of 512 lines with 512 points was used in the areas of each image, captured with Scan Asyst mode. The samples were prepared from the dilution of 1mg GO in 1mL of deionized H₂O and previously sonicated for 4 hours.

The diffraction measurements by X-Ray Diffraction were performed on the Rigaku MiniFlex II diffractometer, varying the scanning at angles of 5° to 50° with a rate of 2° per minute using $\lambda\text{CuK}\alpha$ and monochromator radiation and fixed slots with 30 kV, 15 mA, with the samples powdered at room temperature. From the Bragg Law, $2d\sin\theta=\lambda$, where λ is the wavelength of incident radiation, d is the

distance between atomic planes and θ is the angle of incidence in relation to the plane considered it was possible to calculate the interlamellar distances.

The equipment used for the thermogravimetric analysis of graphite oxide powder was the SDT-Q600 of TA Instrument. The temperature range used in the analysis was 25°C to 1,000°C, with a variation rate of 10°C per minute and in a synthetic N₂ air environment.

The absorption spectrum (FTIR) was obtained from dilute solutions of graphene oxides prepared with a concentration of 1 mg / mL in deionized H₂O and pH > 5. The solution was dripped on a silicon oxide (SiO₂) wafer. The equipment used to obtain these results was the Bruker Vertex 70 Fourier Transform Infrared Spectrometer and it was recorded in the wavenumber range of 750-3,500cm⁻¹.

The software used for almost all characterization was OriginPro 8.5, except for AFM that used for image/histogram processing, the Gwyddion.

5.4 RHEOLOGICAL MEASUREMENTS

Before starting any measurement, the suspensions were kept for constant stirring on a magnetic stirrer at a frequency of 1,000Hz for 10 minutes for homogeneity of the samples as shown in figure 5.6.



Figure 5.6 – The suspensions being stirred on magnet stirrer

The rheological tests of these suspensions of different concentrations were performed on a Physica MCR501 rheometer using the cone-plate geometry with a diameter of 60mm and with a gap of 0.057 mm. The cone-plate geometry consists of a conical shaped body and a planar circular plate shape. The angle of the conical body is generally very small, ie less than 0.01 rad ($\alpha = 6^\circ$). The flow using this type of geometry is homogeneous, since the shear rate is uniform. It can be used for high and low viscosities, and an angular velocity is usually required to measure torque and normal force, or torque is imposed and angular velocity and normal force are measured. This geometry has the advantage that the shear rate is constant throughout the geometry, so it is not necessary to correct the obtained data. However, as with any type of geometry used, the cone-plate presents some limitations such as: edge failure, dispersion, viscous sample dissipation, inertia and sliding on the wall. The problem of sliding on the wall that usually affects the reading of the rheometer in all types of geometry cited can be avoided by using grooved (highly roughened) surfaces.

The other geometry also used to perform some tests despite being in another rheometer (Physica MCR301) to obtain comparative data was the double-gap. The samples are placed in the slots formed by the spacing between the surfaces of the upper concentric cylinders (rotor) which rotates about its axis of symmetry with a certain angular velocity, and lower (body). This technique allows to obtain results with great precision in terms of torque and shear rate, besides the small amount of sample required and time of analysis. The large contact surface area allows the development of studies in which low shear stress measurements are required. (Nakken et al., 2001). Figure 5.7 shows (a) smooth cone-plate separately and (b) cone-plate coupled to the rheometer. And figure 5.8 shows (a) the geometry of double-gap separately (b) the top and bottom cylinder coupled together.

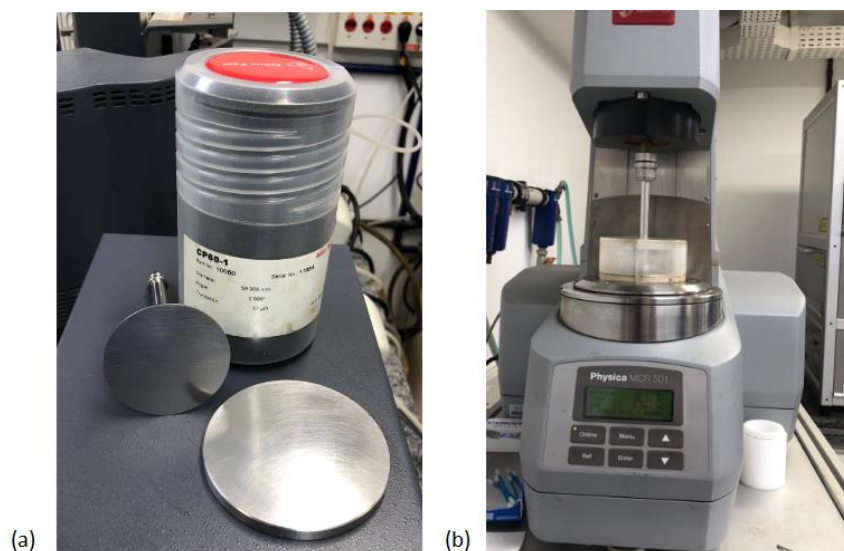


Figure 5.7 – (a) smooth cone-plate separately and (b) cone-plate coupled to the rheometer

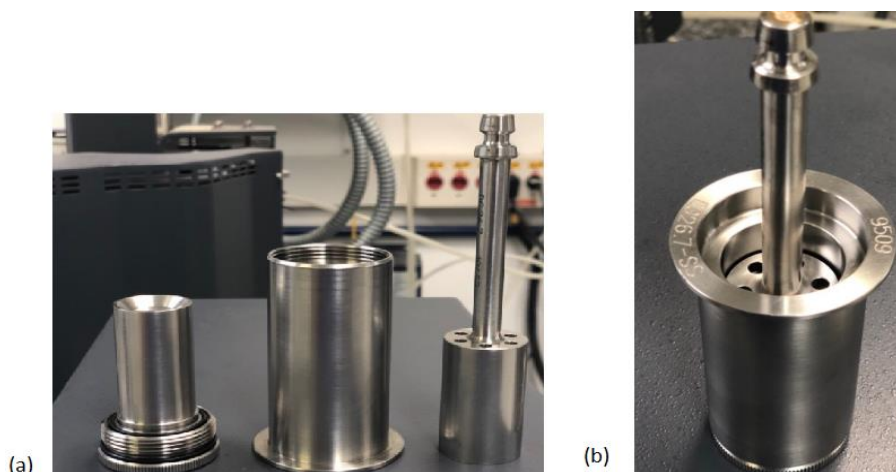


Figure 5.8 – (a) the geometry of double-gap separately (b) the top and bottom cylinder coupled together

MCR501 and MCR301 are stress-controlled rheometer. A protective cap is used above the system to avoid evaporation of the solvent. Each test was repeated at least three times to confirm its reproducibility.

Before starting the measurements, the samples were allowed to achieve the temperature equilibrium of 20°C for 5 minutes. Then, the rotational test is performed in order to obtain the flow curves of the suspension, that is, the evaluation of the behavior of the shear stress and the viscosity as a function of the

shear rate, in steady shear flow. These properties were monitored by ranging the shear rate from $1,000 \text{ s}^{-1}$ to 0.1 s^{-1} .

In these measurements, the flow curve was evaluated decreasing the shear rates from the highest to the lowest, because in this way the time to reach the steady state is lower, since the sample undergoes a pre-shear. Tests were also performed starting from the lowest to the highest rates in order to verify the hysteresis of the curves and if, for these tests, it is necessary to make the pre-shear setting the shear rate.

Tests were also performed to check the stability of the suspensions as follows: first the flow curve was obtained for all concentrations without shaking them and then the samples were agitated and the flow curves were generated. Then, these results were compared on the same graph.

Regarding the oscillatory tests, it was performed the dynamic strain sweep at a fixed frequency of 1Hz ranging the strain from 10% to 10,000%. This result shows the variation of the storage modulus (G') and the lost modulus (G'') as a function of the strain in order to define the linear viscoelasticity region of the suspension, where the modulus (G' and G'') are independent of the amplitude of the deformation. It is also possible to evaluate the fluid behavior in this region, by verifying the predominance of viscous or elastic effects.

Then, for the dynamic frequency sweep, a fixed shear stress value obtained from the linear viscoelasticity region (LVR) was applied, and the frequency was varied from 0.1 Hz to 100 Hz, to investigate the structure of the suspensions. A sinusoidal strain is applied with angular frequency ω and a strain amplitude (in the linear viscoelasticity region) γ_o is imposed:

$$\gamma(t) = \gamma_o \sin(\omega t)$$

The result stress is:

$$\sigma(t) = \sigma_o \sin(\omega t + \delta)$$

Where δ is the phase angle and σ_o is the amplitude of the stress. Due to the viscoelastic behavior of the polymer, the deformation and tension are lagged. If this phase angle is 0° , the material is purely elastic, if it is 90° is purely viscous and if it presents a value between 0° and 90° the material is viscoelastic.

RESULTS AND DISCUSSIONS

This chapter presents the results obtained through the characterizations and rheological measurements in order to better understand the morphological and structural characteristics resulting from processing methods and the analyzes made on the basis of these presented results to understand the influence of nanostructures on the properties of material such as mechanical, thermal and rheological properties.

By analyzing the product obtained in the volumetric flask after the oxidation of the two methods (which were distinguished only by the oxidation time) it was possible to notice a difference in the coloration of the reaction of graphite with acids, where the GrO obtained with 96h of oxidation presented lighter color in relation to the GrO obtained with 2h.

6.1 STRUCTURE CHARACTERIZATION OF GRAPHENE OXIDE

The characterizations were made through the techniques of X-Ray Diffraction (XRD), Raman Spectroscopy, Thermogravimetric Analysis (TGA), Atomic Force Microscopy (AFM) and Fourier Transform Infrared (FTIR).

6.1.1 X-RAY DIFFRACTION

This technique is used to evaluate if the chemical treatments preserved the structure of the graphite and GO lamellae. X-Ray Diffraction evaluates the nanoparticles at the structural level thus allowing an analysis of the exfoliation of the graphene oxide (GO). The greater the interplanar spacing between the layers of graphene oxide, the better oxidized is the GO obtained. The interplanar distance is interpreted in a diffractogram as follows: The further to the left the peak is displaced, the greater the interplanar distance.

It is possible to observe in figure 6.1 that the two methods had a great difference in the crystallographic distance of the material. According to Bragg's

Law, the material with 96 hours of oxidation obtained a greater spacing between the basal planes of 9.066 angstroms (\AA), than in the material with 2 hours of oxidation and the graphite. The graphite showed a peak at the 2θ of 26.2° relative to the plane, which indicates a distance between layers of 3.12 angstroms. In the GO of 2h, the peak occurred at 2θ of 9.9° , which shows that the spacing between layers became 8.935 angstroms. The possible cause of the greater distance in the GO of 96h is the availability of time that the material had for the entrance the functional groups in its structure, besides the water adsorbed during the process.

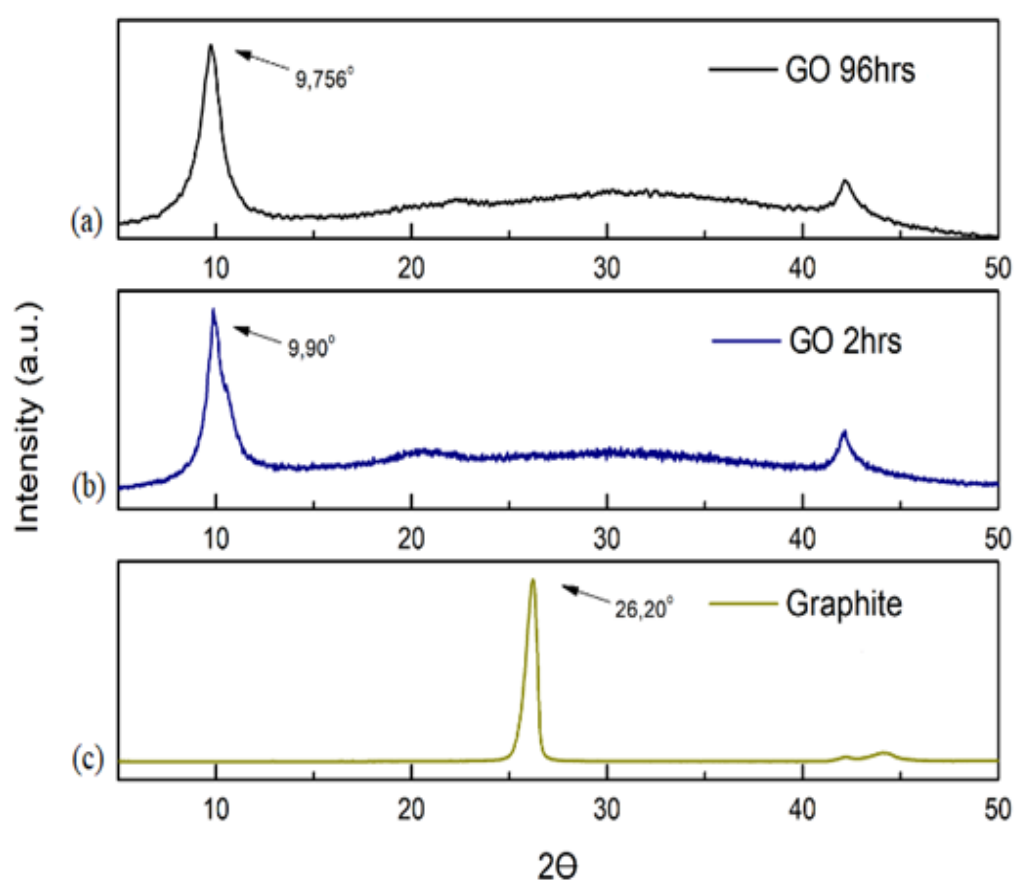


Figure 6.1- XRD interference planes for (a) GO 96h (b) GO 2h and (c) Graphite

6.1.2 RAMAN SPECTROSCOPY

For the analysis of the results provided by Raman, it is necessary to understand the Raman spectrum. The Raman spectrum provides several bands, but the most important ones for carrying out the study and characterization of the load are the D, G and 2D bands. The D band refers to the amount of defects in the carbonaceous structure and incomplete bonding of sheets edges, the G band is related to the stretch vibrations between sp^2 carbon pairs and the 2D band provides information about the existence of multilayers in the sample.

In the Raman spectrum, according to figure 6.2, characteristic peaks such as the D-band between $1,300$ and $1,500\text{cm}^{-1}$, which corresponds to the edge defects and the defects in the graphite layers that arise during the oxidation due to the addition of functional groups. This growth is due to the emergence of incomplete bonds, heteroatoms attached to the sheets structure and change of the sp^2 to sp^3 bond type in some carbon atoms. The small peak in the D-band of graphite facilitates the oxidation process by the modified Hummers method.

It is also possible to observe the predominance of the G band between $1,500$ - $1,750\text{cm}^{-1}$ in the graphite spectrum, which is related to the vibrations created by the elongation of the sp^2 bonds between the carbons and which means that its crystalline structure presents a small amount of structural disorder. With the oxidation process, there was a widening of the G band indicating a greater disorder in the graphical structure and a greater heterogeneity.

The 2D band between $2,500$ - $2,750\text{cm}^{-1}$ is related to the two-dimensional structure of the material and provides information on the existence of multilayers in the sample appearing only in the structure of the graphite.

The I_D/I_G intensity ratio of the D and G bands allows an estimation of the structure disorder or defects. For the GO with 96h of oxidation, $I_D/I_G = 1.109$. Comparing with the GO with 2h of oxidation, which has an $I_D/I_G = 1.066$, it can be concluded that the graphene oxide produced with a greater number of hours of oxidation had more defects introduced in its structure, defects produced by the introduction of a greater number of functional groups in the structure. As the oxidation time increased, there was an increase in the D-band peak and a decrease in the 2D-band peak, indicating that there was damage in the carbonaceous structure and the disintegration of the graphene layers composing the graphite.

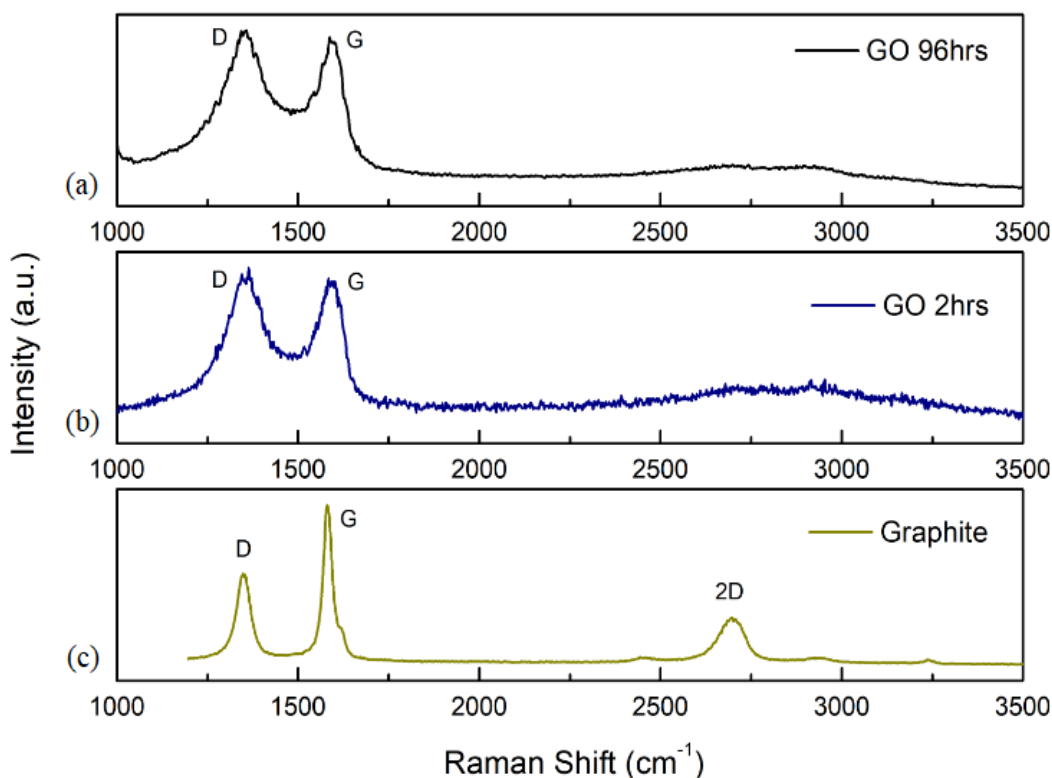


Figure 6.2- Raman spectrum of the (a) GO 96h (b) GO 2h and (c) Graphite

6.1.3. THERMOGRAVIMETRIC ANALYSIS

Thermogravimetric Analysis, although not producing images as the branch of microscopy, reveals important characteristics of materials related to thermal stability, study of decomposition, oxidation, reaction equilibrium, water loss, and heat transmission, among others. Mass losses and heat flow are associated with phase transitions and reactions in the material in the temperature range studied.

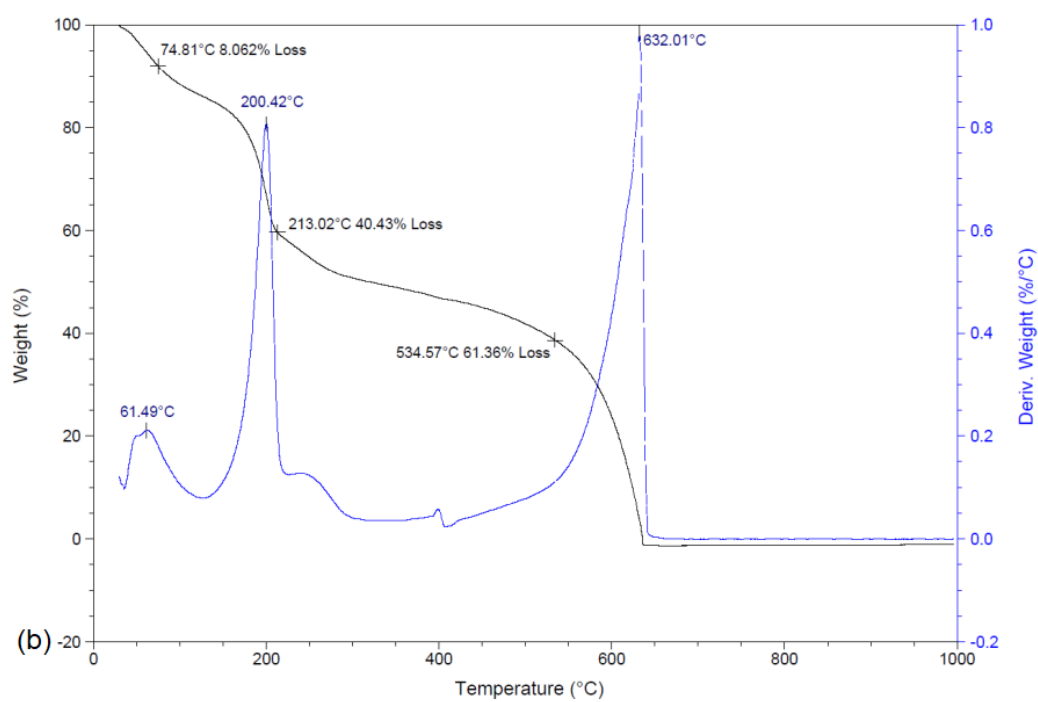
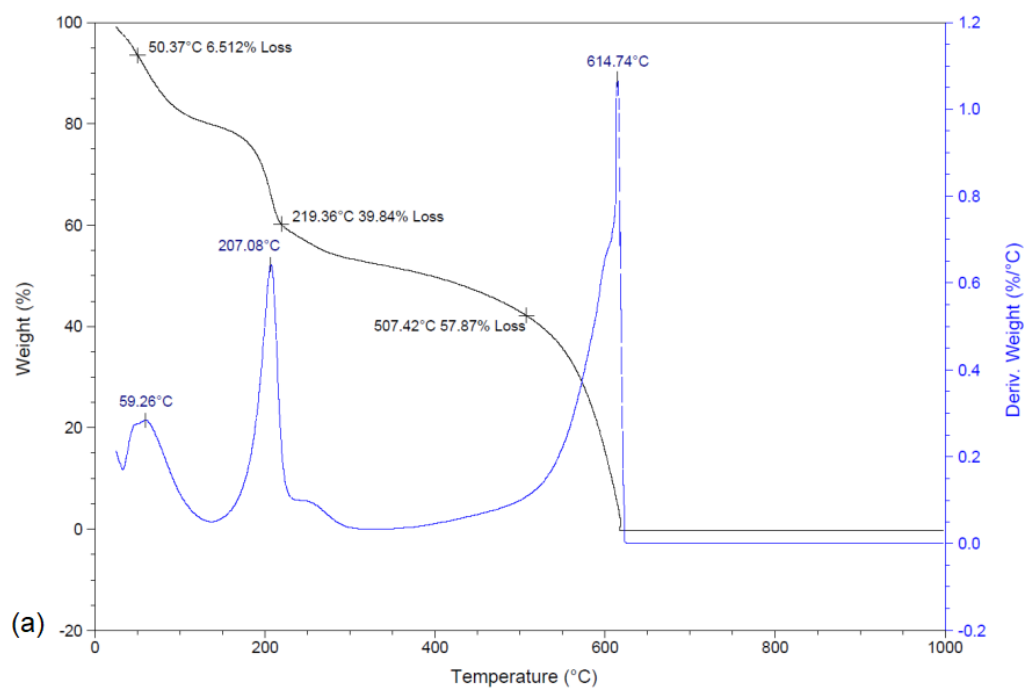
The thermogravimetric curve represents the loss of mass with increasing temperature. According to figure 6.3 (a), it is possible to notice a small loss of mass up to the temperature around 51°C, resulting from the loss of residual moisture absorbed by the material during the exfoliation process. At around 219°C, a further sharp drop corresponding to a loss of 40% of the material mass is observed and is related to the loss of the groups that were introduced into the material during oxidation. Finally, the sample has a gradual loss of mass around 507°C, related to the process of degradation of the graphite structure. The dTG of the first point shows the most significant variation around 59°C. The peak loss of oxygenated

groups occurred at approximately 207°C and the loss of graphitic material had the highest rate of change at 614°C.

Regarding to figure 6.3 (b), at approximately 75°C there is a loss of 8% of mass, resulting from the loss of residual moisture from the exfoliation process. At 213°C, the 40.43% mass loss is related to the loss of oxygenated groups that were introduced into the material during oxidation. The remainder shows the mass loss of the graphite material. The dTG shows the derivative of the percentage mass loss as a function of temperature. Represents where the largest variation in the rate of mass loss occurs. In the case of the GO 96h sample, the first point representing water loss had a more significant variation around 61.49°C. The peak loss of oxygenated groups occurred at approximately 200°C and the loss of graphitic material had the highest rate of change at 632°C, where after this variation there is no more burning, because the nitrogen used in the analysis cannot burn the residual carbon.

Graphite has only one peak in dTG as it has no oxygenated groups and / or adsorbed water to lose. The peak mass loss indicates that the temperature at which the graphite burn rate is at its highest change is 861.81°C, with onset and offset temperatures at 731°C and 893°C respectively.

These values indicate that the GOs are thermally unstable and that the system with the highest oxidation time obtained the largest amount of functional groups introduced in the graphite structure. While Jiang et al. (2000) showed that graphite, regardless of size, is thermally stable because of its high structural stability.



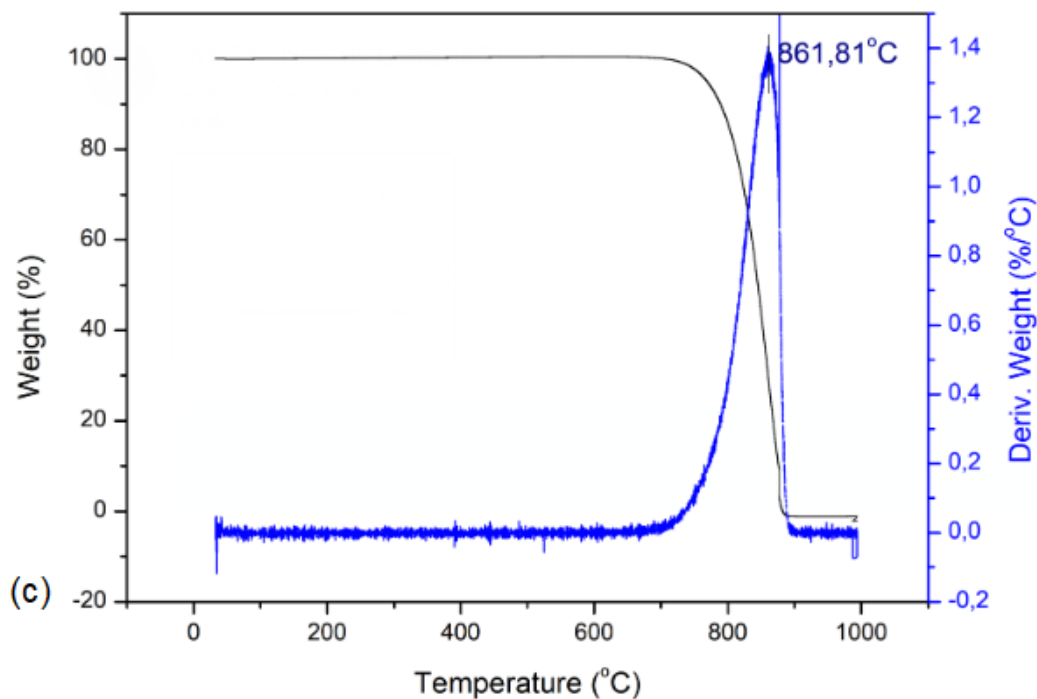


Figure 6.3- Thermogravimetric curves for (a) GO-2h and (b) GO-96h oxidized (c) graphite

6.1.4 ATOMIC FORCE MICROSCOPY (AFM)

The responses of Atomic Force Microscopy (AFM) can come in the form of images that allows sizing the stacking of the sample sheets, or in the form of graphs that allows detecting the degree of oxidation of the sample through the particle size. The AFM was the characterization technique that allowed to observe more clearly the structural difference between the GO obtained with the different oxidation times.

The graphs shown in figure 6.4 show the sheets are still overlapping having several different thicknesses and that the oxidation level influenced the particle size, since the GO of 2h has particles ranging their size from 5 to 145 nanometers and the GO of 96h had particles with size from 0 to 60 nanometers, most of which are concentrated in the 0-40 nanometer range and other points exceeding 60 nm do not belong to the sample and may be external particles present at the time of the test. The AFM for the grafite was not performed because the particle is larger than 3 micrometres (has 45 micrometres) and is considered too large to be used in AFM.

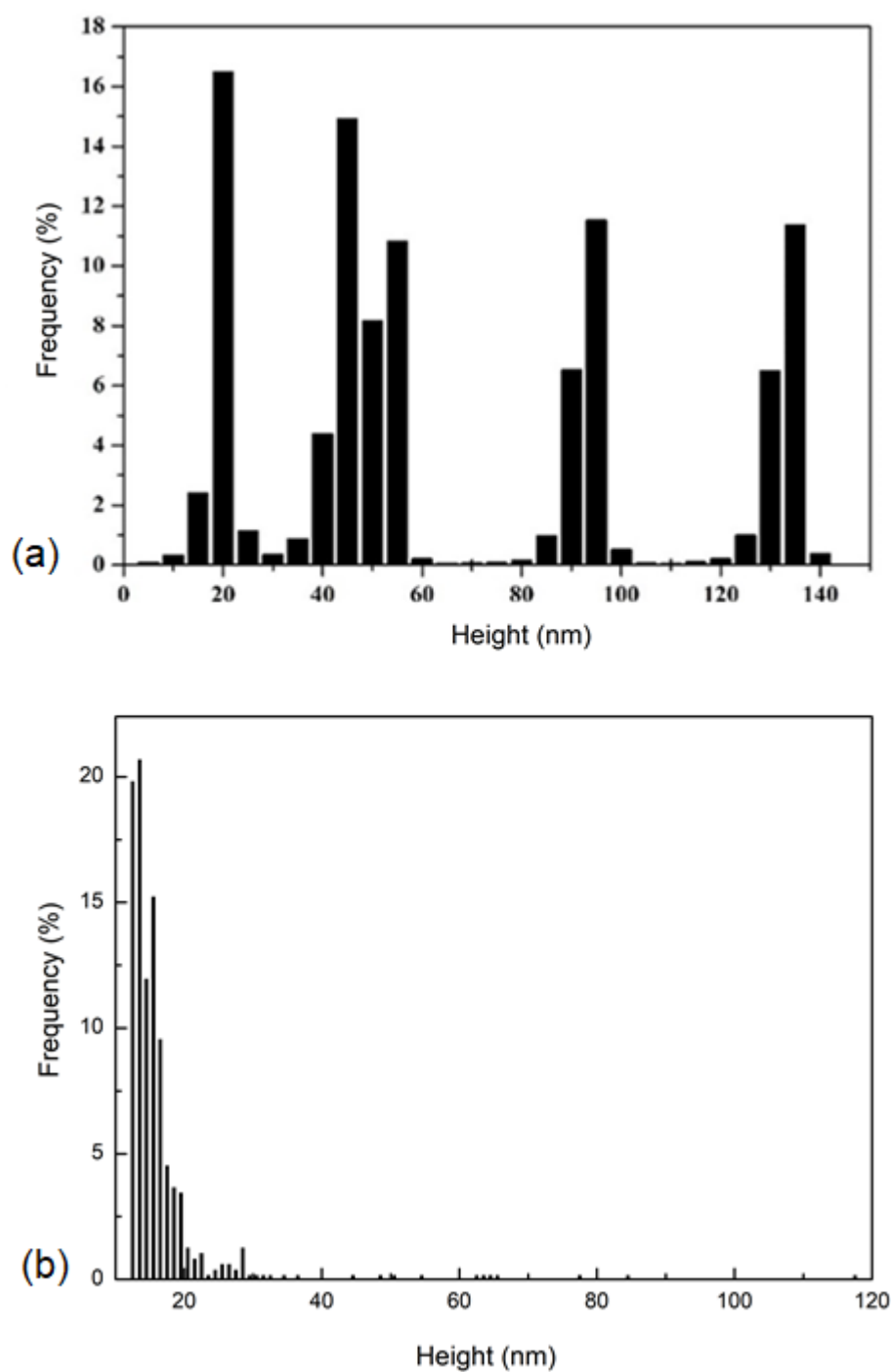


Figure 6.4- Frequency (%) of GO sheets of (a) 2h of oxidation (b) 96h of oxidation as a function of their height.

6.1.5. FOURIER TRANSFORM INFRARED (FTIR)

Infrared spectroscopy consists of the vibrations of the atoms present in a given structure. In the conventional infrared spectrum, only the vibrations that influence the rhythm of the dipole moment of the molecule will be investigated, being possible to verify the presence of oxygenated groups in the GO lamellae resulting from the oxidation process. Figure 6.5 shows the FTIR spectrum of the oxidized GO with 2h and 96h. Kartick et al. (2013) proved in their work that the graphite FTIR spectrum does not present significant peaks.

In FTIR spectrum of GO-2h, high absorption is observed in the region of 3,400 to 2,400 cm^{-1} indicating the presence of OH group, this absorption usually overlaps the C-H stretch. The band located at 1,718 cm^{-1} has a base value for absorbing type C=O bonds. Combined with the absorption at approximately 1,048 cm^{-1} indicating the C-O group vibration, the presence of groups such as carboxylic acids, ester, aldehydes and ketones may be indicated. The peak at 1,624 cm^{-1} represents the energy absorption of carbon vibrations in aromatic arrangement.

GO-96h's spectrum is very similar to GO-2h's. It can be observed a strong absorption between 3,400 and 2,400 cm^{-1} , which normally overlaps the CH stretch, due to the presence of the OH group. Analyzing an absorption peak at approximately 1,710 cm^{-1} for C = O stretching vibrations, it is possible to detect the presence of functional groups such as carboxylic acid, ether, ester (these three groups can be estimated when taken into account also the presence of absorption at 1,093 cm^{-1}), ketone and aldehyde (a weak peak is observed at 2,900 ~ 2,800 cm^{-1}). The absorption with media intensity indicated between 1,418 ~ 1,352 cm^{-1} takes into account the torsion vibration of carbon-hydrogen bonds in the GO structure.

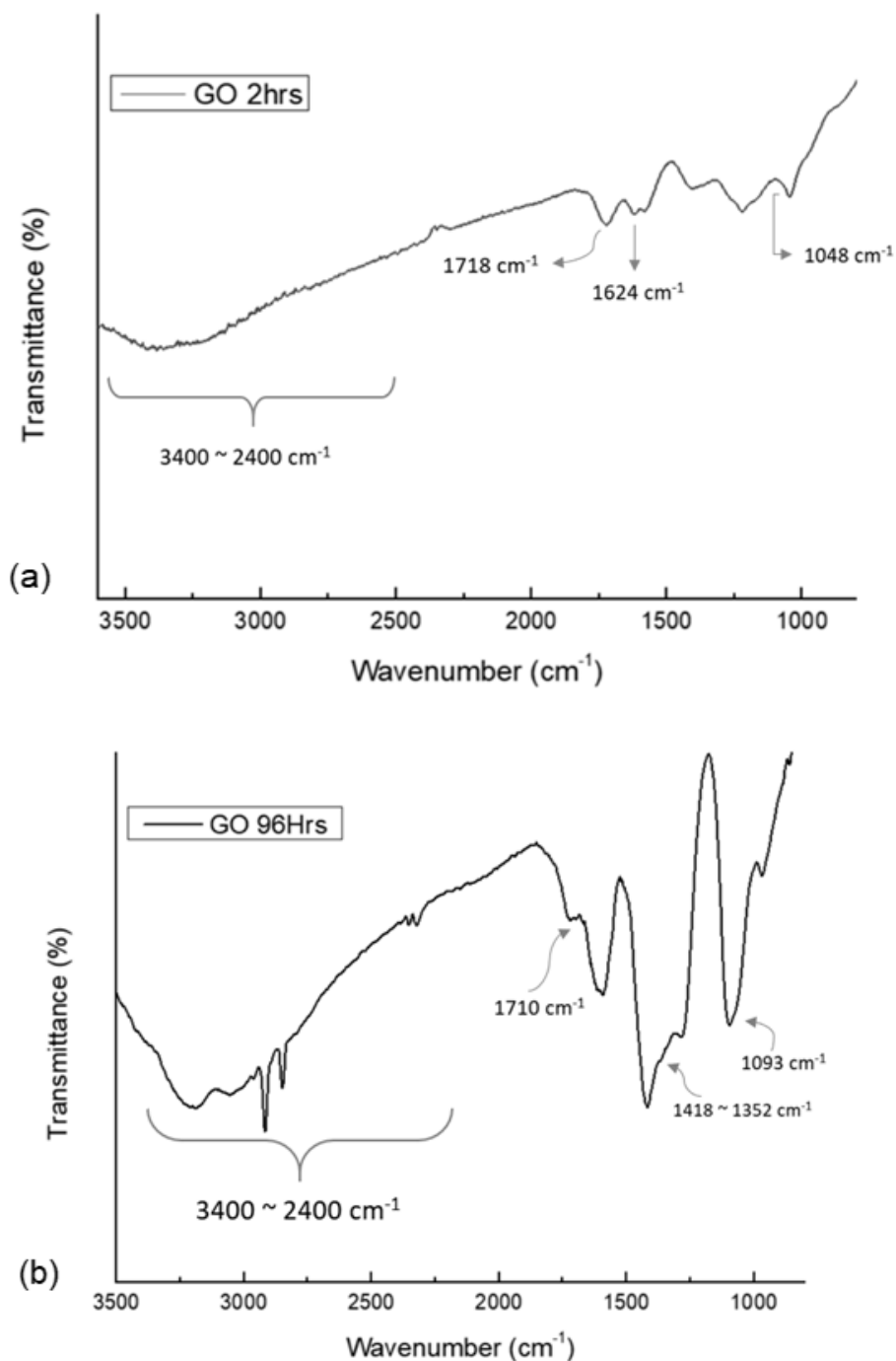


Figura 6.5 – FTIR spectrum of GO with (a) 2h (b) 96h of oxidation.

The results obtained through these characterization techniques presented similar properties to the GO values obtained in other studies in the literature, thus showing that the graphene oxide obtained by the modified Hummers method was satisfactory. It was also possible to notice that the GO obtained with the highest oxidation time (96h) presented less thick sheets due to a larger insertion of

oxygenated groups between the layers. This may be justified by the fact that these groups further damage these sheets and facilitate their separation in the exfoliation process in the ultrasonic bath.

From the analysis of Atomic Force Microscopy (AFM), it was concluded that it was not possible to obtain exactly the thickness of a GO sheet that is around 0.8nm (Oliveira, 2019), so the closest that was possible to reach was a GO with multilayers, ie multilayers Graphene Oxide (mGO).

And, upon these concluding observations, rheological tests were performed to evaluate how these GO sheets obtained with different oxidation times are able to interfere with the PEG 400 rheological properties for possible future applications.

6.2 RHEOLOGY OF GRAPHENE OXIDE SUSPENSIONS IN POLY(ETHYLENE GLYCOL)

Another way to verify if the GO was successfully obtained was by preparing aqueous dispersions of GO-2h with concentration of 10mg/ml according to tests found in the literature and comparing the rheological results. Figure 6.6 shows the results of the rotational tests of the aqueous GO dispersion prepared with 10mg/ml GO-2h.

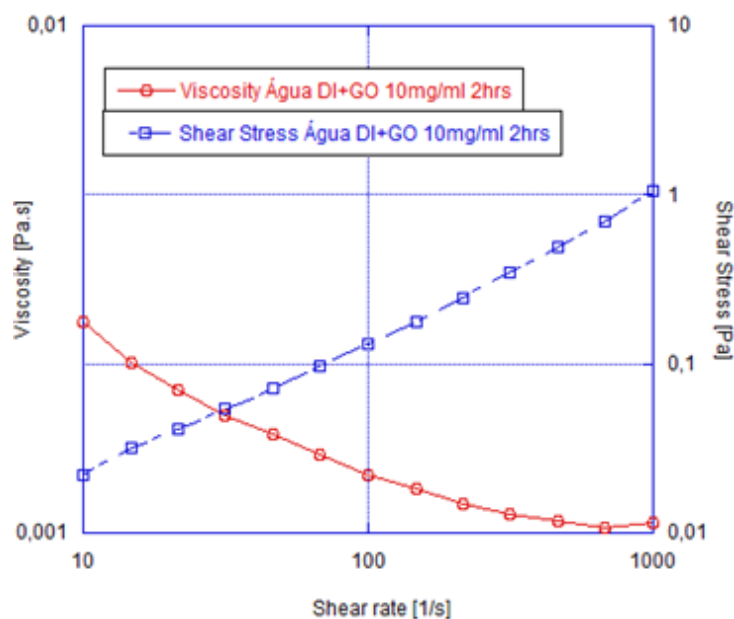


Figure 6.6 – Flow Curve of aqueous dispersion with 10mg/ml of GO-2h

Analyzing Figure 6.6 and comparing the results found in the paper entitled Colloidal and Rheological Behavior of Aqueous Graphene Oxide Dispersions in the Presence of Poly (ethylene glycol) by Shu et al. (2015) it was possible to observe that the viscosity and shear stress curves as a function of the shear rate had the same behavior and the same values within the analyzed range from 10 to 1,000s⁻¹.

The difficulty of achieving a stable dispersion has been a major challenge for researchers when there are no chemical changes such as pH change or surfactant addition. To solve this problem, homogenization of the dispersion is carried out by stirring techniques, such as the ultrasonic bath, magnetic stirrer and high pressure homogenizer. Factors such as intensity and time of stirring are also able to influence the effect of dispersion.

In order to analyse the stability of the dispersions, tests were performed with and without agitation. In Figure 6.7 these tests are shown for the graphene oxide suspensions of 2 hours of oxidation in PEG with respective concentrations of 0.1, 1, 10, 20 and 80 mg/ml. It was possible to observe that at low shear rates the samples did not demonstrate well-defined rheological behavior while at high rates where the sample is being stirred the behavior of the suspensions obtained consistent and plausible results. This demonstrates the fact that these samples, because they have particles that deposit in the bottom of the fluid, need to be agitated to avoid sedimentation problems that make the rheometer difficult to read.

Through these tests, it was possible to conclude that all tests would need to be agitated before they can be started.

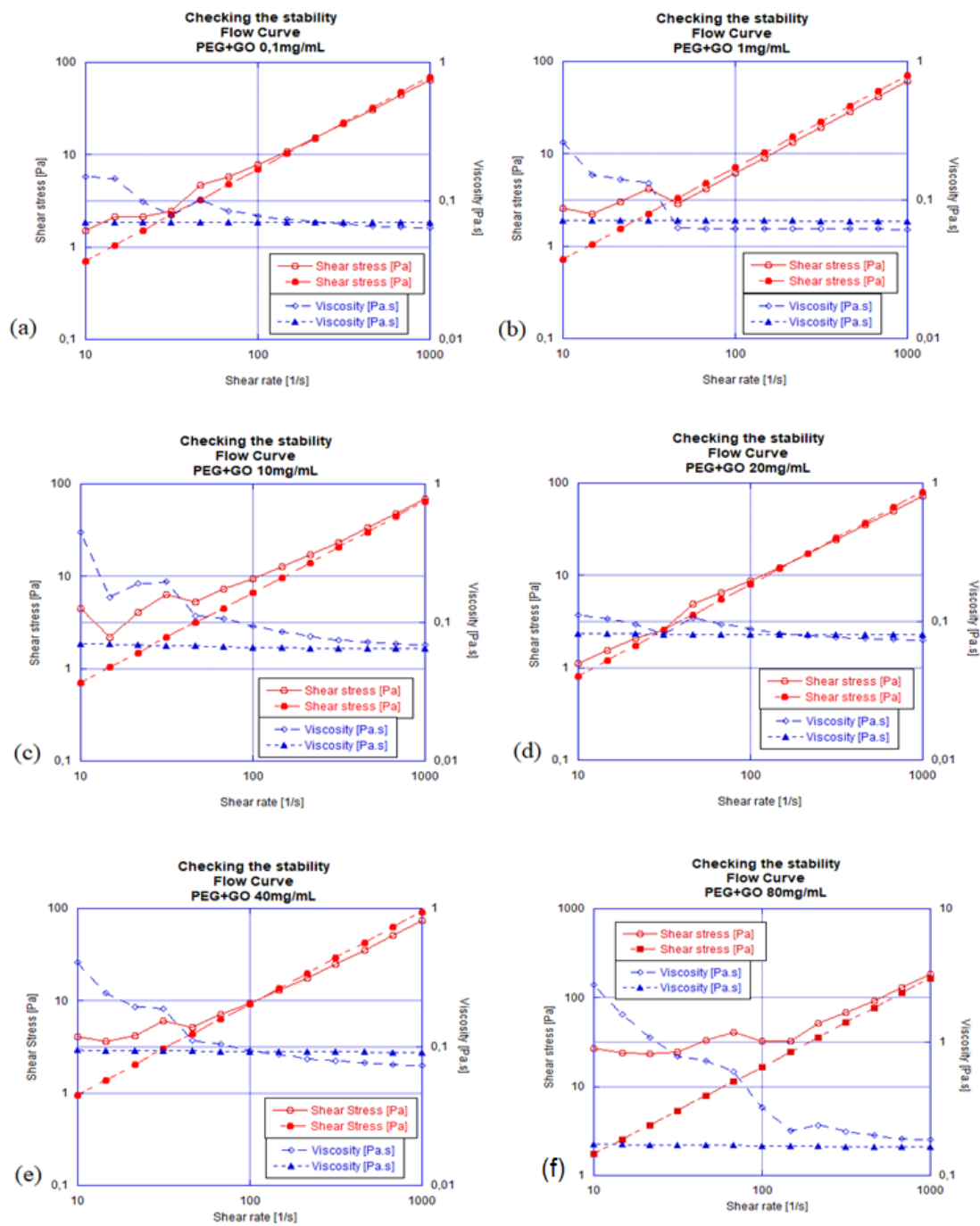


Figure 6.7 – Stability tests for suspensions with concentrations of (a) 0.1 (b) 1 (c) 10 (d) 20 (e) 40 and (f) 80 mg/ml of GO-2h comparing suspensions with agitation (filled symbols) and without agitation (open symbols).

Pre-shear was performed in order to determine the time the sample took to achieve the steady state regime. In Figure 6.8 it is possible to observe pre-shear tests, where a shear rate of 10s^{-1} was set for all tests (tests made with a shear rate less than 10s^{-1} obtained responses with random points, because for these low shear rates the torque obtained was below the minimum torque required by the rheometer) and the behavior of the viscosity as a function of the shear time was evaluated. With these tests it was possible to observe that for all the samples, the time to reach the steady state regime was very small, thus demonstrating that the sample did not need to be pre-sheared for the beginning of the tests of the flow curves.

Tests made with the intention of obtaining the flow curve usually evaluate the curves from the highest to the lowest shear rates so that the test generally occurs relatively faster, because this way, the sample undergoes a pre-shear causing all particles of the fluid to depart from the same point and the time taken to reach steady state becomes shorter. In many cases, when tests are started from the lowest to the highest rates, the time taken to perform the test becomes longer. However, as the pre-shear tests showed that the sample reached steady state in a few seconds, to confirm these results, flow curves were obtained for each sample applying a shear rate of 10 to $1,000\text{s}^{-1}$ (without pre-shearing the sample) and then 1,000 to 10s^{-1} and compared their execution times. Figure 6.9 shows that there was no hysteresis between the flow curves generated for all the concentrations made with the GO obtained with 2 hours of oxidation and that the test took the same time to run both ways, thus corroborating the results observed in the pre-shear, demonstrating that the sample did not need to be pre-sheared.

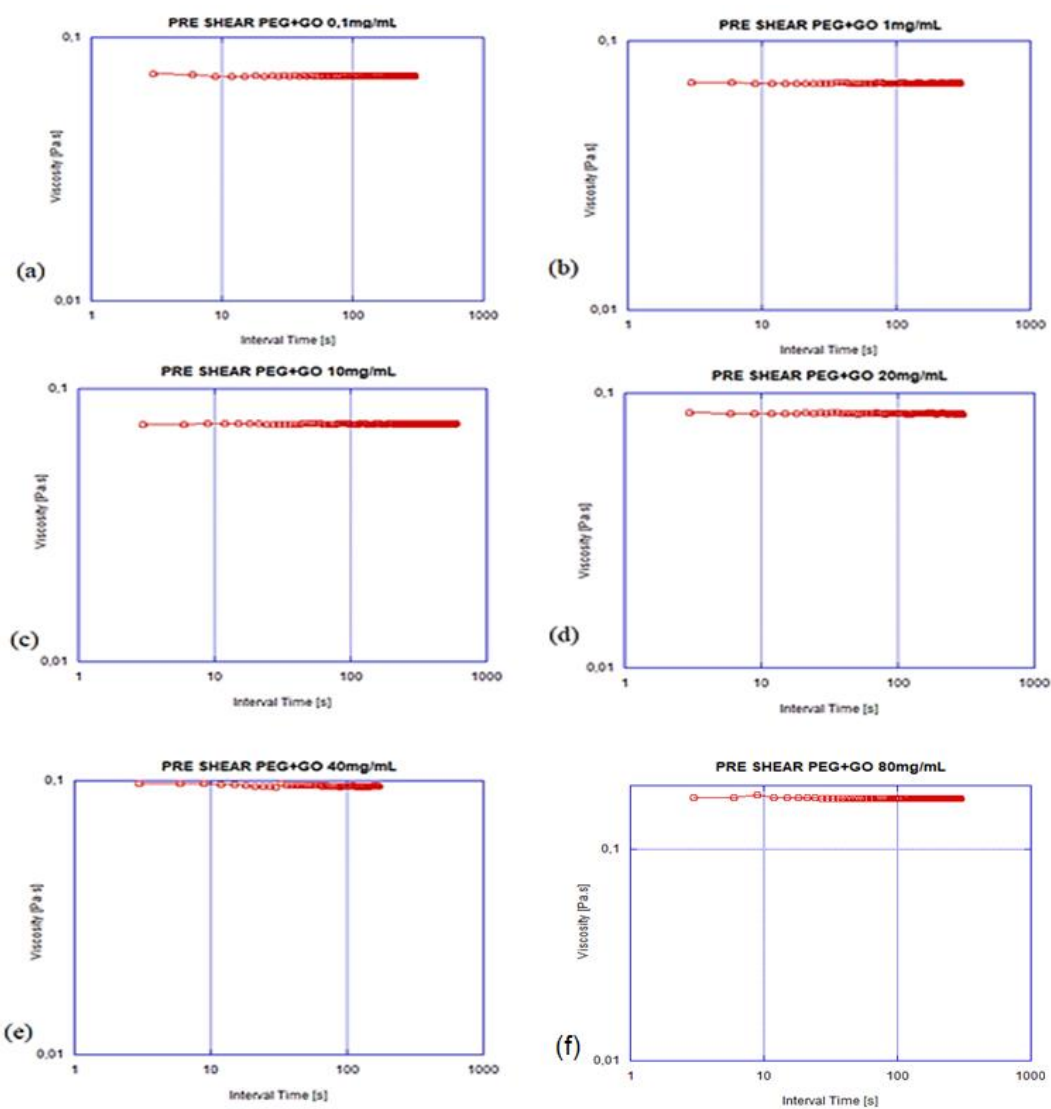


Figure 6.8 – Pre-shear of GO-2h suspensions in polyethylene glycol with (a) 0.1 (b) 1 (c) 10 (d) 20 (e) 40 and (f) 80mg/mL.

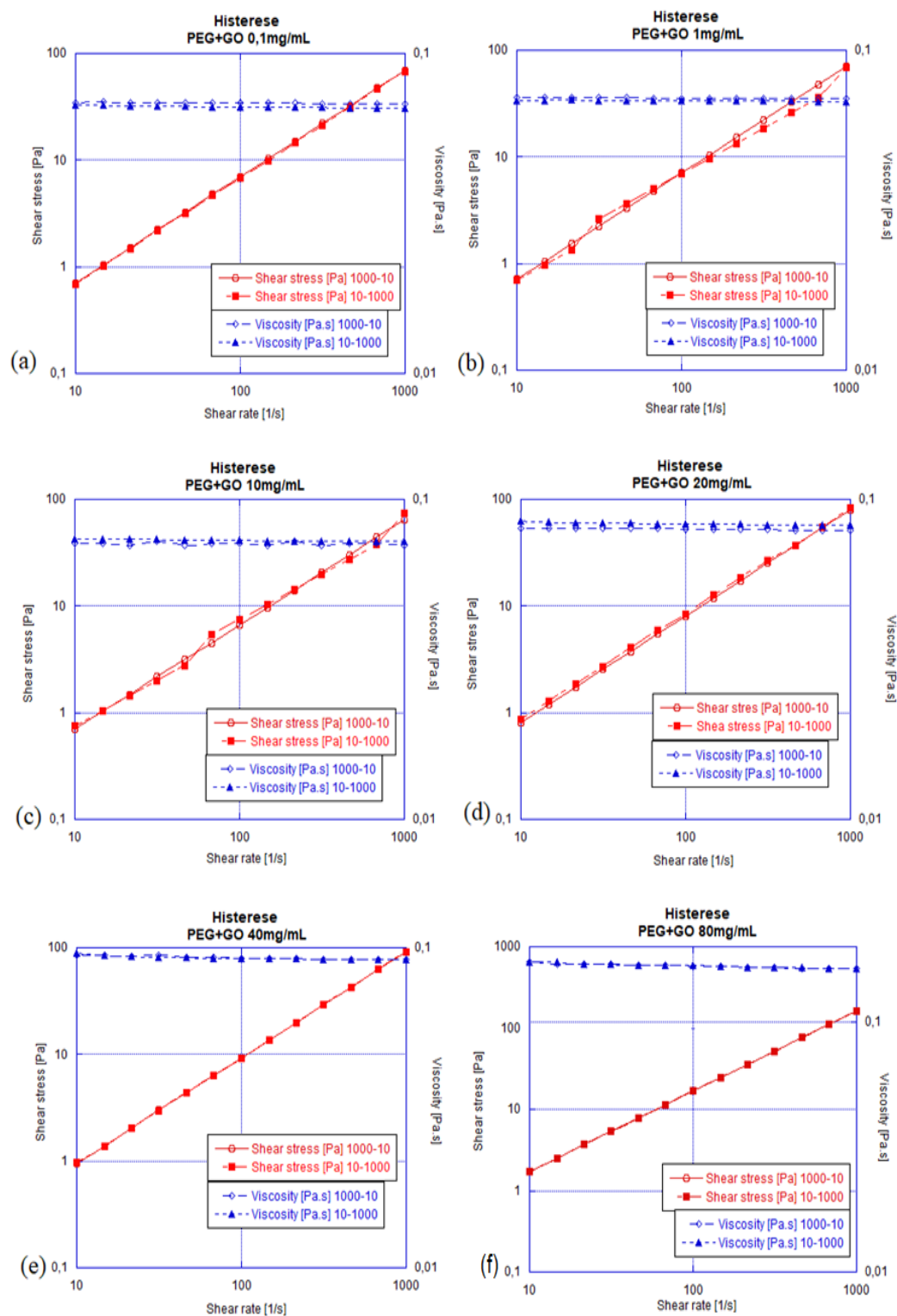


Figure 6.9 – Flow curve applying a shear rate of 10 to 1,000s⁻¹ (without pre-shearing the sample) and then 1,000 to 10s⁻¹ for suspensions with concentrations of (a) 0.1 (b) 1 (c) 10 (d) 20 (e) 40 and (f) 80mg/ml of GO-2h.

GO concentration and oxidation level may influence the rheological properties of graphene oxide suspensions, so it is necessary to investigate rheological behavior by varying concentrations using shear rates ranging from 0.01 to $1,000\text{s}^{-1}$ to cover a large variety of applications.

The tests performed on a steady state shear flow were used to investigate the flow properties of the material by recording the shear stress and viscosity at increasing shear rates. Points not shown in the graphs showed lower torque values than the minimum reliable torque in the respective geometry.

Figure 6.10 shows the viscosity behavior as the shear rate increases of suspensions with GO concentration of 40mg/mL obtained with the oxidation times of 2h and 96h and it was observed the viscosity is higher in the 96h oxidation GO suspension than in 2h.

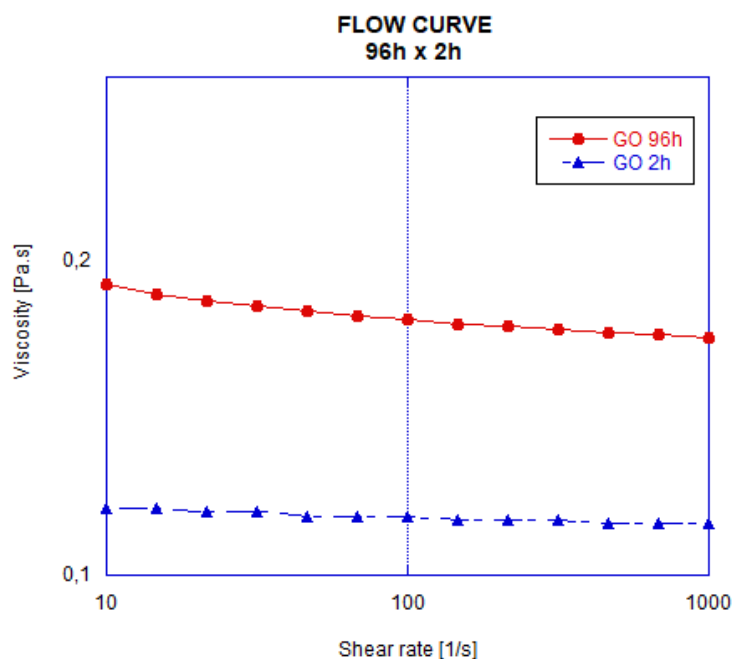


Figure 6.10 - Flow curve comparing viscosity for suspensions with 40mg/mL of GO with different oxidation times

The results demonstrated that the oxidation levels influenced the viscosity. The GO particles have an extremely large specific surface and can interact with a large amount of polymer in suspension. Thangavel and Venugopal (2014) evaluated different levels of GO oxidation in their work and concluded that the highly oxidized GO had a higher interaction capacity than the lower oxidized GO. The reason that interaction rates increase as the oxidation rate of GO increases is due to

the increase of negatively charged molecules in hydrophilic functional groups. The basic mechanism of interesting rheological behavior is the Bridging effect. Because of the size effect, multiple particles are connected by the intrachain bridge of a polymer. Wang et al. (2004) confirmed, through the tubeless siphon technique that one factor that can lead to increased viscosity of a polymer solution is the addition of nanoparticles to the solution, this is justified by the fact that the extension of polymer bridges between the particles increases flow resistance.

Summarize, The increased viscosity observed with increasing oxidation time can be explained by the fact that the longer the oxidation time, more oxygenated groups are inserted into the graphite structure and these sheets are exfoliated easier getting smaller, as observed in the AFM and Raman spectrum results. This results in a greater interaction between the nanoparticles and the polymer (this interaction is made by hydrogen bonds), where the PEG chains are connected on the GO sheets forming larger aggregates in the shaped of a network that restricts the suspension mobility and lead to an increase in viscosity, which explains the so-called Bridging effect. Figure 6.11 shows the Bridging effect. Thus, the GO obtained with 96h of oxidation was more strongly oxidized as evidenced by the TGA, causing the viscosity of the suspensions made with this GO to be higher than the GO obtained with 2h of oxidation.

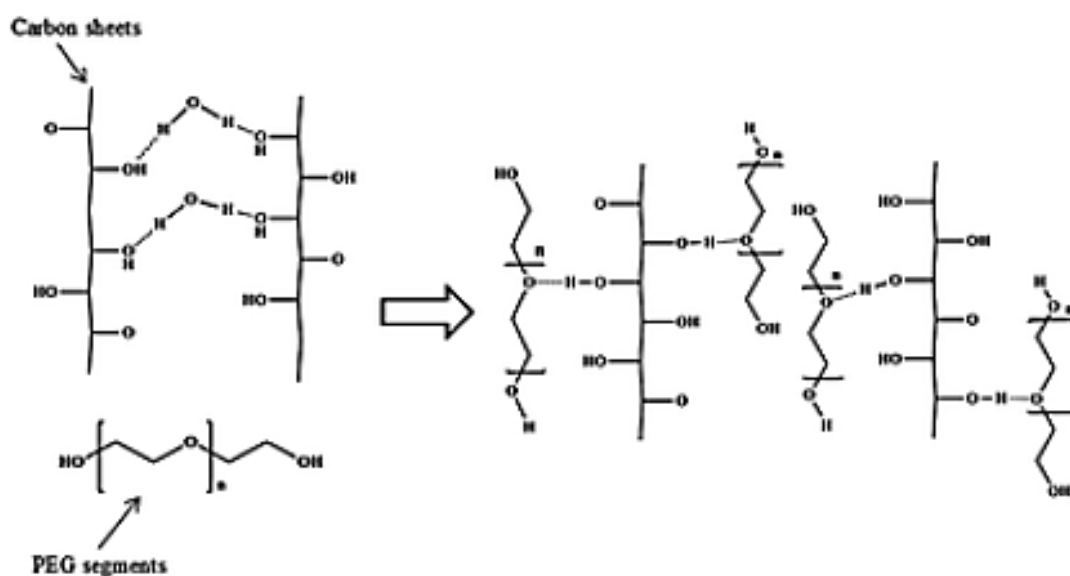


Figure 6.11 – Bridging effect (Wang et. al., 2012)

In figure 6.12 it can be noted that for both oxidation times there is an increase in viscosity as the concentration is increased. According to Kamibayashi et al. (2008), generally, increasing particle concentration slowly generates an increase in suspension viscosity. Einstein's theory of suspension rheology says that the distortion of the velocity field in the surroundings of each particle induces an increase in viscosity, because the addition of particles inevitably generates an increase in liquid viscosity.

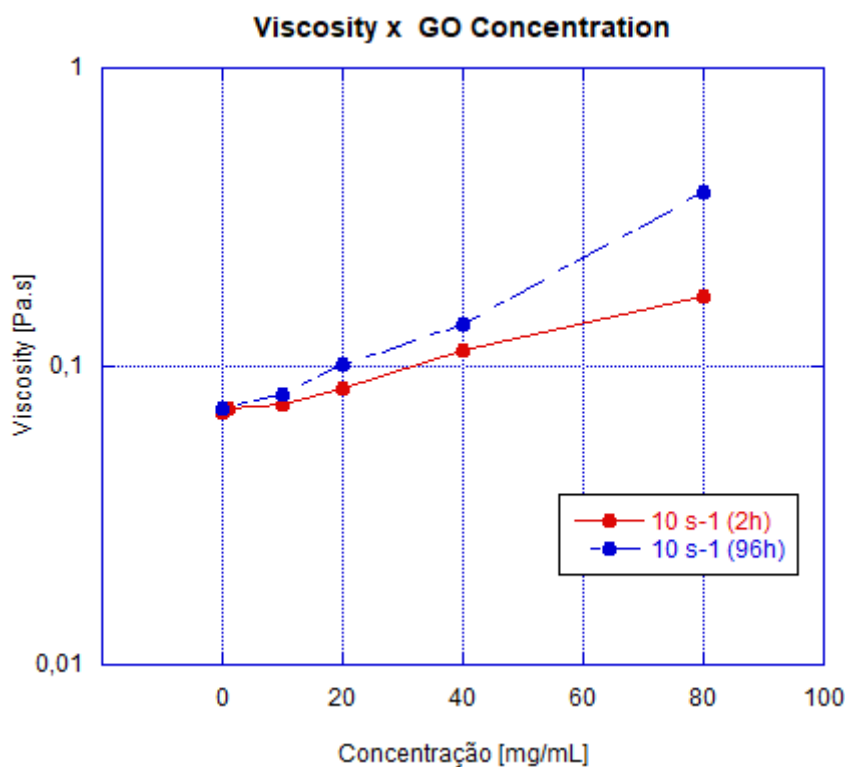


Figure 6.12 – Shear viscosity of suspensions of GO as a function of different GO concentrations at shear rate 10s^{-1}

The rheological behavior of these observed suspensions can be discussed in terms of the networks formed between GO nanoparticles and the polymer by the Bridging effect already explained previously. As can be seen from figure 6.13, at rest, these networks are kept structured. As a shear rate begins to apply, the network structure is broken and these particles are oriented along the flow direction.

Figure 6.14 shows that in the flow curve of the GO of 96h the change of the Newtonian behavior to a pseudoplastic behavior begins to be observed at suspensions with concentration of 40mg/ml, whereas in the tests made for concentrations of 0.1 to 80 mg/ml of GO-2h all samples presented a Newtonian behavior in the shear rate range analyzed. The pseudoplastic behavior (shear thinning) observed in suspensions with a concentration of 40mg/ml upwards made with GO-96h is justified by the decrease in viscosity as the shear rate increases. This behavior is related to the deinterlacing and orientation of the polymeric chain, together with the slip/orientation of the shear GO layers (Giannelis, 1998).

According to Shu et al. (2016), the above isotropic-nematic phase transition phenomenon can be explained as follows. The isotropic phase (molecules have no fixed position and orientation) is observed in suspensions with very low concentrations of GO, as the sheets of GO are individually dispersed in the polymer with weak interaction among them, so the rheological behavior of the GO suspensions is Newtonian. When the GO concentration is above a critical concentration, the GO suspensions can turn into a nematic liquid crystal (the molecules have a certain orientational order), exhibiting a characteristic shear-thinning behavior under constant shear flow.

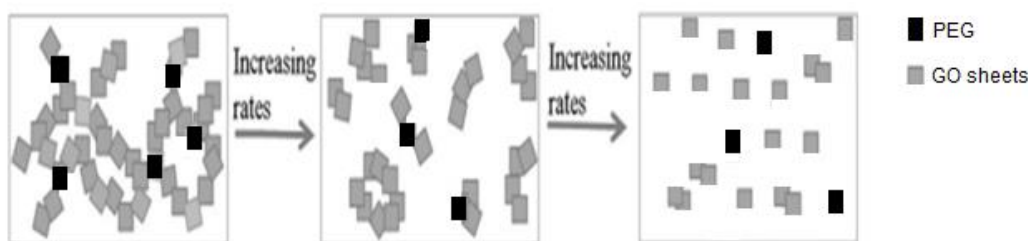


Figure 6.13 – Schematic representation of the breakdown of the structure into flocs, with decreasing sizes as the shear rates increase
(adapted from Vallés et al., 2014)

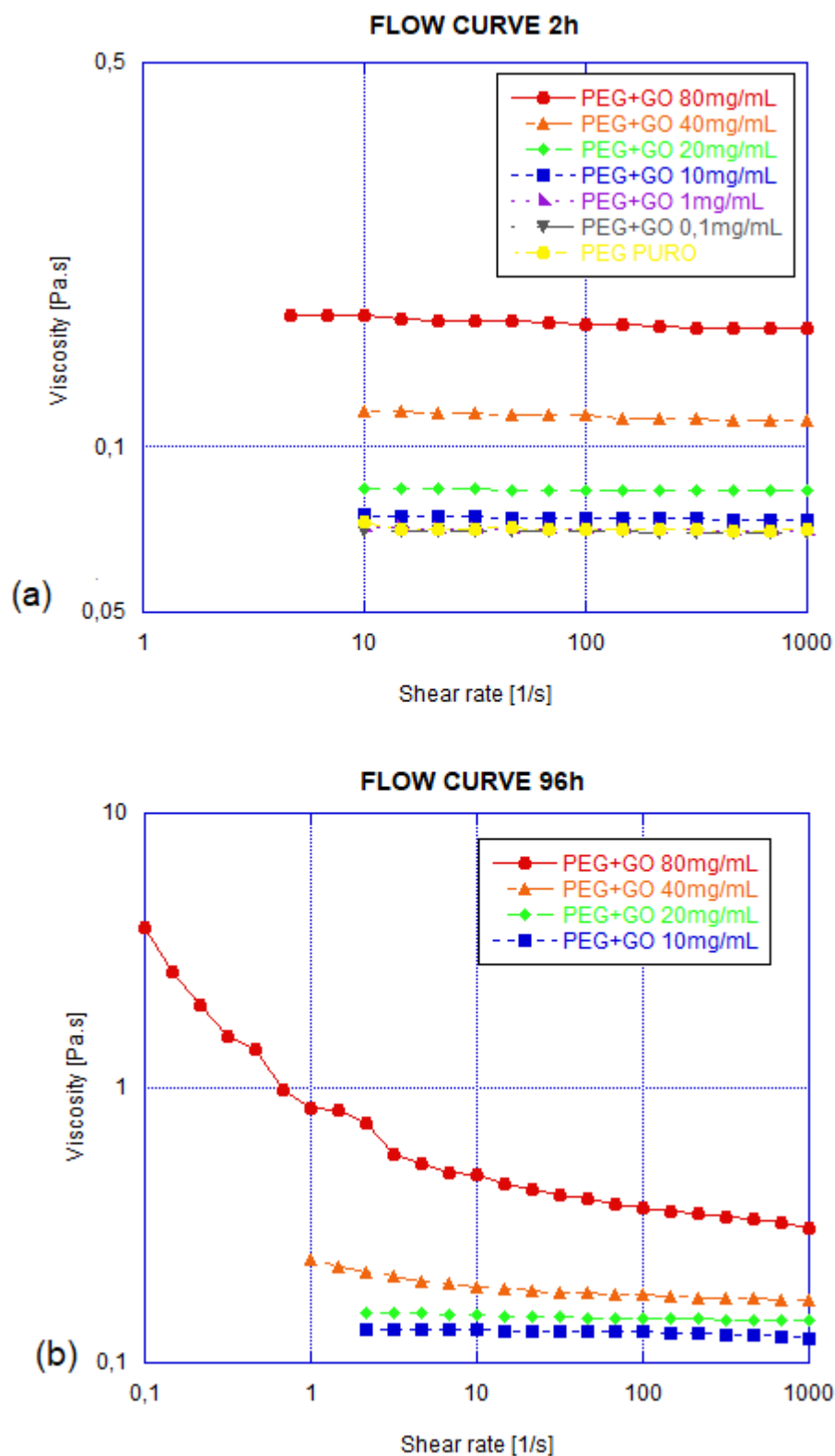


Figure 6.14- Steady shear rate flow behavior of the (a) GO of 2h (b) GO of 96h of oxidation

Oliveira (2010) observed that the addition of nanoparticles in homopolymers (polymer formed by only one monomer, as for example, polyethylene glycol) causes changes in viscoelastic behavior causing the viscous and elastic characteristics of pure polymer to differ, depending on nanoparticle type, affinity and degree of dispersion.

Small amplitude oscillatory shear (SAOS) can detect the dynamic mechanical response of complex fluids near equilibrium state. Typical curves as a function of angular frequency (ω) of dynamic storage (G') and loss modulus (G'') for GO suspensions with different concentrations can be determined.

Several works have been done dealing with the rheological behavior of graphene oxide dispersions focusing on the characterization of viscoelastic behavior of this fascinating material. In aqueous suspensions with concentration of GO below the critical concentration ($c_g \sim 6 \text{ mg / mL}$) it was observed that the modulus G' and G'' are apparent frequency dependent, suggesting that GO dispersions behave as viscoelastic fluids. According to Naficy et al. (2014), As these suspensions increase the concentration of these nanoparticles and approach the critical concentration, a frequency dependent plateau-like behavior is being observed as direct consequence of sheets being trapped by their neighbours preventing the stress relaxation on the longest time-scale of the measurement resulting in greater packaging of the nematic phase. In tests with suspensions with concentration above the critical concentration, these modulus begin to lose this dependency with frequency and the storage modulus increasing much faster than the loss modulus, indicating a solid-like behavior. (Giudice and Shen, 2017; Naficy et al., 2014; Shu et al., 2016).

The characteristic flow behavior of GO dispersions is fundamentally different from those associated with usual viscoelastic materials, including polymers. The generic properties reported in these work concluded above can be considered as a universal guideline for processing different GO dispersions based on their rheological properties.

In linear oscillatory shear flow, strain sweep tests were performed, as shown in figure 6.15, in order to obtain the linear viscoelastic region that serves as input data for the frequency sweep test. The strain value was determined to be applied for oscillatory frequency sweeps, in order to use the same value for all samples and to

avoid influences concerning the test parameters on the rheological behavior of the samples. It is also possible to observe through the strain sweep that the suspensions do not have a yield stress, since there is no crossover between the values of the storage and loss modulus.

When choosing a strain value that is within the linear viscoelastic range for all tests, this value was set, and a frequency sweep of 0.1 to 100Hz was done. Low frequency sweep to analyze the response of nanoparticles dispersed in nanofluids and high frequency to analyze the response of the nanofluids polymer matrix. Values below 0.1 Hz have been discarded because they have a very low torque value, and values above 100Hz are also discarded because the phase angle is not between 0 and 90°, and the material structure could be beginning to break.

Figure 6.16 shows the behavior of the G' and G'' modulus as the frequency increases. For 2h GO tests, from pure polymer to 40mg / mL suspension, the viscous modulus does not differ significantly presenting values very close to all concentrations and the elastic modulus is practically negligible compared to the viscous modulus value, meaning that the material does not present elasticity. While the 80mg/mL suspension began to show slight signs of elasticity. This may be justified by the fact that at low concentrations, GO sheets are randomly dispersed in the polymer and the increase in concentration was too insignificant to cause severe effects on the loss modulus as the dominant part was still the polymer. For the 96h GO tests, it can be observed that the suspension with 80mg/mL GO concentration started to show viscous modulus values slightly higher than the suspensions with the other concentrations and the elastic modulus started to increase significantly, this may lead to the conclusion that the suspension of GO 96h with 80mg/mL concentration is close to the critical concentration, as long as the formation of the nematic phase of liquid crystals is completed, an additional increase in volume fraction results in the simultaneous increase of both modulus, with the storage modulus increasing much faster than the loss modulus.

Comparing the modulus responses obtained for each oxidation time as shown in figure 6.17, it was possible to note that the suspensions presented values close to the viscous modulus, but the suspension made with the GO with a higher oxidation time obtained a higher elastic modulus response, a fact that may be justified because the more oxidized GO has a greater interaction with the PEG compared to the less

oxidized GO. This can best be seen by comparing the prepared suspensions with a concentration of 40mg /mL.

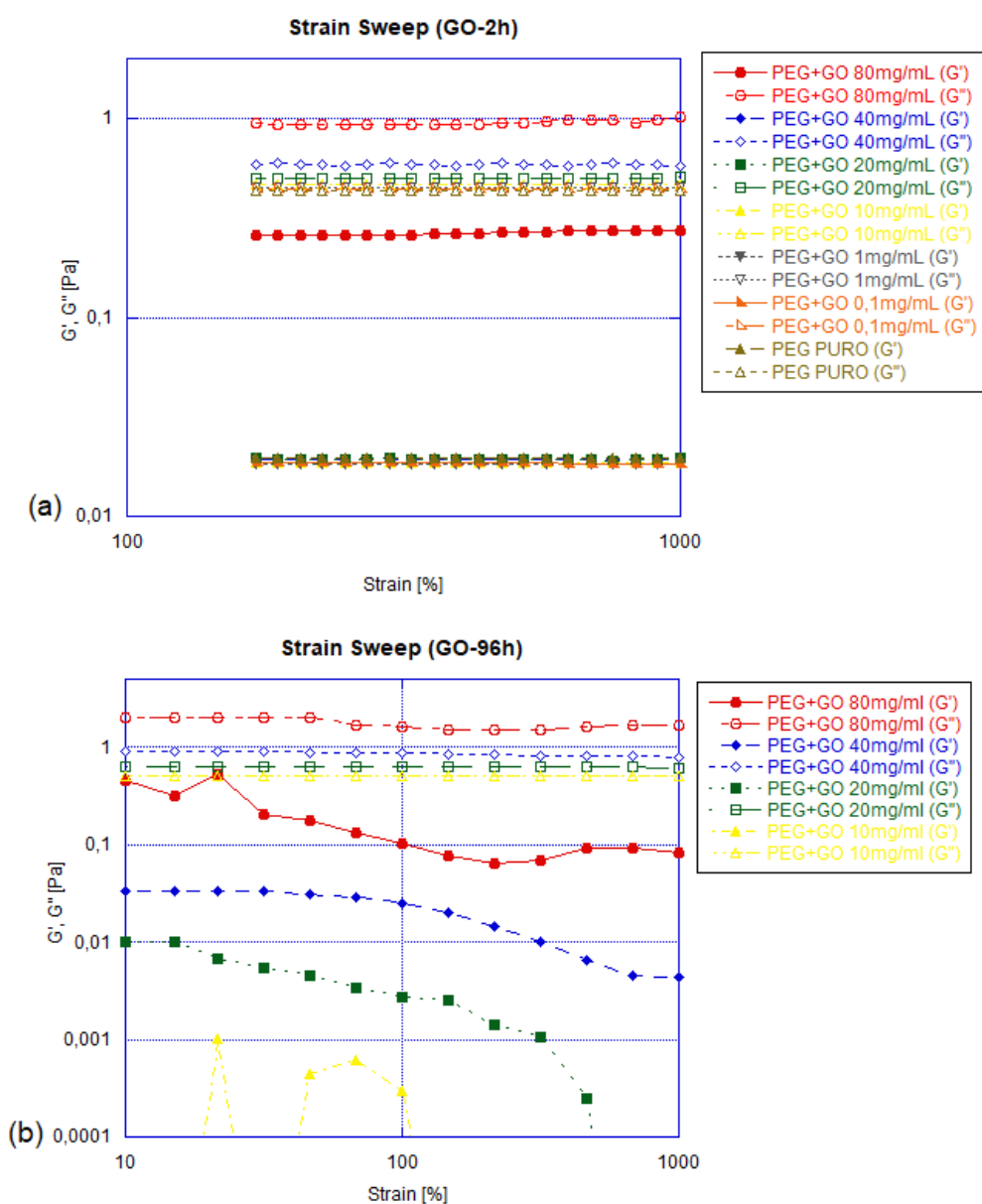


Figure 6.15 – Strain sweep for (a) GO of 2h (b) GO of 96h of oxidation

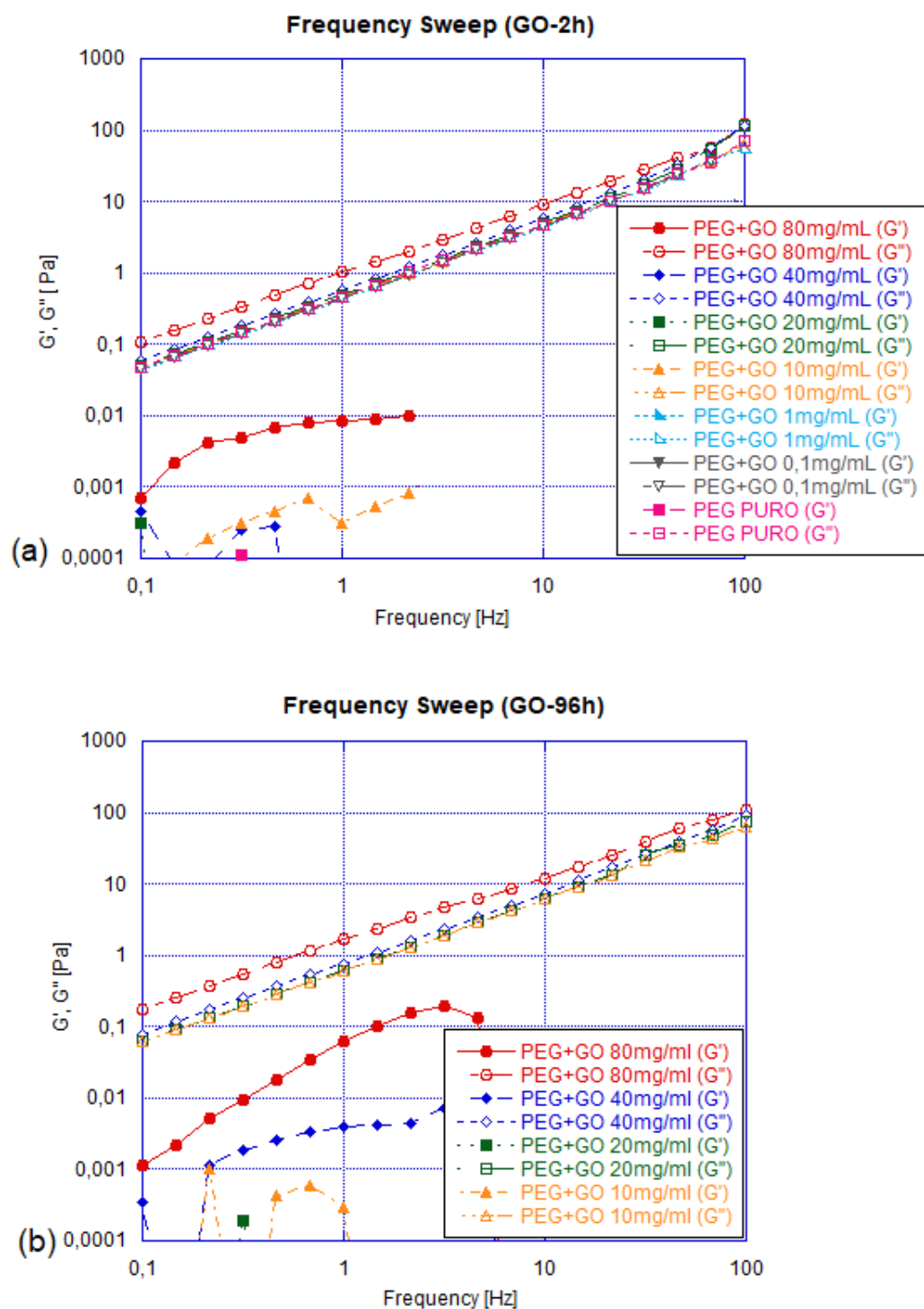


Figure 6.16 – Frequency Sweep for (a) GO of 2h (b) GO of 96h of oxidation

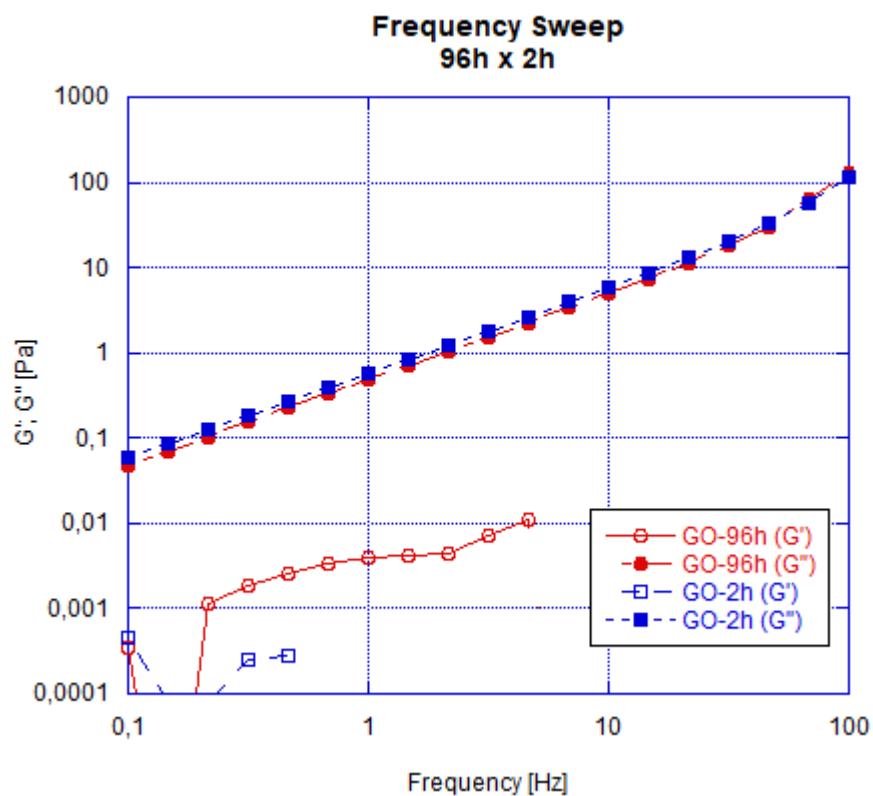


Figure 6.17 - Comparison of viscous and elastic modulus between suspensions with 40mg/mL of GO made with 2h and 96h of oxidation

7

CONCLUSIONS

The results indicated that the method of obtaining GO via the modified Hummers method was efficient, since it presented similar properties to those predicted in the literature and reference material. The degree of oxidation directly influenced the exfoliation process of the graphite coverslips.

The X-Ray Diffraction technique that assesses nanoparticles at the structural level was responsible for proving that the GO-96h had a greater interplanar distance between the layers than the GO-2h. In the Raman spectrum, with the increase of the D bands and decrease of the 2D band as the oxidation time increased, it was possible to notice that there was increased damage to the carbonaceous structure and disintegration of the graphene layers that compose the graphite. With the FTIR and TGA tests, it was possible to notice the presence of oxygenated groups in the graphite structure and with the AFM that the 96h GO presented smaller particles than the GO prepared with 2h oxidation.

Thus, through the characterization techniques used in this work, it was possible to prove that the oxidation occurred and that the longer the oxidation time, the greater the number of functional groups introduced in the graphite structure increasing interplanar distances thus facilitating the process of exfoliating the coverslips resulting in decreased crystal size.

The rheological analyzes showed that the addition of GO in the polyethylene glycol (PEG) contributed significantly to change in the viscosity values of the suspension. The factors of this change are related to the charge concentration and oxidation level of the obtained GO particles.

Regarding the oxidation level, the GO obtained with higher oxidation time presented higher viscosity value compared to the less oxidized GO, because the higher the amount of oxygenated groups inserted in the graphite structure, the easier these particles were exfoliated and interact with the chains of the polymer restricting the mobility of the suspension and increasing flow resistance. And regard to charge

concentration it was also possible to notice an increase in viscosity with the increase of nanoparticles in the suspensions.

The rheological tests also allowed to investigate the dependence of the suspension viscosity with the shear rate, where it was possible to observe the change from Newtonian to pseudoplastic behavior of the GO suspensions prepared with 96h of oxidation as the concentration increases. Moreover, through the oscillatory tests, it was possible to verify that only the most concentrated 96-hour GO suspensions showed elasticity.

These results obtained from steady state shear tests and SAOS frequency sweep serve to understand the interaction between nanostructure and the mechanical response of GO / PEG or GO / other polymers suspensions and provide some guidelines for nanofluid production.

In the present study, the only parameter of the GO obtaining process that was varied and its morphological, structural and rheological alterations were analyzed was the oxidation time. And as the oxidation time, other parameters such as the types of oxidizing agents used, the type of graphite, the sonication time, among others can also influence the characteristics and properties of the obtained GO and, therefore, must be analyzed.

As a suggestion for future works focusing on this type of research aiming to improve and gain more knowledge regarding the properties of graphene oxide suspensions, studies on extensional flow rheological characterization should be further explored because this type of regime has great importance in flows with large variations in area, such as flows in extrusion processes, regularly found in industrial operations.

Other topics that may be interesting to work are: doing a solution analysis of GO in AFM because rheological tests are done with suspensions, evaluating the effect of temperature on rheological properties because increasing temperature leads to breakdown of hydrogen bonds, perform tests with PEG of other molecular masses to evaluate how the brige effect may interfere in the viscosity of these suspensions and perform tests by adding salts to verify the change in the rheological behavior of the suspensions caused by these salts, as they neutralize the negative charges present in the molecules.

REFERENCE

AVILA, E. S., MELO, C. C. N., SAMPAIO, T. P. and MACHADO, F. M. **“Síntese e caracterização de óxido de grafeno e óxido de grafeno reduzido”** (2017). Revista Brasileira de Engenharia e Sustentabilidade, v. 3, n. 1, 19-24.

BARNES, H. A., HUTTON, J. F., WALTERS, K. **“An introduction to rheology”** (1989). Elsevier, vol. 3, Rheology series.

BRETAS, R. E. S.; D’ÁVILA, M. A. **“Reologia de Polímeros Fundidos”** (2000). São Carlos, Editora da UFSCar.

BORDONI, C. B. **“Estudo de catálise com grafeno, para degradação de fenol produzido em refinarias”** (2014). Monografia do Departamento de Engenharia de Petróleo – Universidade Federal Fluminense, Niterói.

BOTAN, R., NOGUEIRA, T. R., LONA, L. M. F. AND WYPYCH, F. **“Síntese e caracterização de Nanocompósitos Esfoliados de Poliestireno - Hidróxido Duplo Lamelar via polimerização in situ”** (2011). Polímeros vol. 21 no.1.

CAMARGOS, J. S. F., SEMMER, A. O. and SILVA, S. N. **“Características e aplicações do grafeno e do óxido de grafeno e as principais rotas para síntese”** (2017). The Journal of Engineering and Exact Sciences, vol. 3, n. 08, 1118-1130.

COSTA, C. M. **“Caracterização reológica de fluidos complexos”** (2017). Pontifícia Universidade Católica, Rio de Janeiro, Brasil.

COUTINHO, F. M. B., MELLO, I. L. and MARIA. L. C. S. **“Polietileno: principais tipos, propriedades e aplicações”** (2003). Universidade Estadual do Rio de Janeiro, Rio de Janeiro, Brasil. Polímeros vol. 13. No. 1.

CRUZ. M. C. P. **“Influência do poli(etileno glicol) (peg) no processo de microencapsulação da oxitetraciclina no sistema alginato/quitosana: modelamento "in vitro" da liberação oral”** (2004). Tese do doutorado do curso de engenharia química – UNICAMP, Campinas.

DAS, P. K. **“A review based on the effect and mechanism of termal conductivity of normal nanofluids and hybrid nanofluids”** (2017). Elsevier, Journal of Molecular Liquids, 240, 420-446.

FERREIRA, A. M.; SILVA, K. L. S. and ANDRADE, R. J. E. **“Estudo reológico do óxido de grafeno com diferentes níveis de oxidação”** (2018). Universidade Presbiteriana Mackenzie, São Paulo.

FIM, F. D. C. **“Síntese e popriedades de nanocompósitos de polietileno/nanolâminas de grafeno obtido através de polimerização in Situ”** (2012). Universidade Federal do Rio Grande do Sul, Porto Alegre.

GAN, Y., SHU, R., TAN, D., XING, H., XU, G. and YING, Q. **“Colloidal and rheological behavior of aqueous graphene oxide dispersions in the presence of poly(ethylene glycol)”** (2016). In journal Elsevier, Colloids and Surfaces A: physicochemical and engineering aspects, pp.154-161.

GANGWAR, P., MAITI, U., EUN LEE, K., KIM, S. **“Rheological properties of graphene oxide liquid crystal”** (2014). Carbon. 80. 453. 10.1016/j.carbon.2014.08.085.

GIUDICE, F. D. and SHEN, A. Q. **“Shear rheology of graphene oxide dispersions”** (2017). Elsevier, Current Opinion in Chemical Engineering, 23-30.

HERMANY, L. **“Aproximações estabilizadas de escoamento de fluidos viscoplásticos através de uma expansão seguido de uma contração axissimétrica”** (2012). Dissertação de Mestrado do curso de engenharia mecânica – UFRS, Porto Alegre.

IMPERIALI, L.; LIAO, K.H.; CLASEN, C.; FRANSAER, J. and MACOSKO, C. W. **“Interfacial Rheology and structure of tiled graphene oxide sheets”** (2012). Langmuir, 28, 7990-8000.

JALURIA, Y. **“Fluid Flow Phenomena in Materials Processing – The 2000 Freeman Scholar Lecture”** (2001). Journal of fluids engineering, New Jersey.

JIANG, W., NADEAU, G., ZAGHIB, K. and KINOSHITA, K. **“Thermal analysis of the oxidation of natural graphite – effect of particle size”** (2000). Elsevier, Thermochimica Acta, 351, 85-93.

JUNIOR, M. A. P. A and LOBATO A. K. C. L. **“O Grafeno: meios de obtenção e possíveis aplicações na indústria automotiva”** (2017). UNIFACS, Salvador.

KARTICK, B., SRIVASTAVA, S. K. and SRIVASTA, I. **“Green Synthesis of Graphene”** (2013). Journal of nanoscience and nanotechnology, vol. 13, 4320-4324.

KAMIBAYASHI, M. OGURA, H. and OTSUBO, Y. **“Shear-thickening flow of nanoparticle suspensions flocculated by polymer bridging”** (2008). Elsevier, Journal of Colloid and Interface Science, 321, 294-301.

KASHYAP, S., MISHRA, S. and BEHERA, S. **“Aqueous Colloidal Stability of Graphene Oxide and Chemically Converted Graphene”** (2014). Journal of Nanoparticles. 2014. 10.1155/2014/640281.

KONIOS, D.; STYLIANAKIS, M. M.; STRATAKIS, E. and KYMAKIS, E. **“Dispersion behaviour of graphene oxide and reduced graphene oxide”** (2014). Elsevier, Journal of Colloid and interface Science, 430, 108-112.

KRISHNAMOORTHY, K., VEERAPANDIAN, M., YUN, K., KIMA, S. **“The Chemical and structural analysis of graphene oxide with different degrees of oxidation”** (2013). Carbon. 53. 38-49. 10.1016.

LACERDA, L. M. **“Grafeno, o material do futuro”** (2015). Universidade Geraldo Di Biase, Volta Redonda.

LIPSON, H and R. STOKES, A. **“A New Structure of Carbon”** (1942). Nature. 149. 328-328. 10.1038/149328a0.

LOMAX, D. J., KINLOCH, I. A., VALLES, C. and YOUNG, R. J. **“The rheological behavior of concentrated dispersions of graphene oxide”** (2014). In Springer, J Mate Sci, 49: 6311-6320.

MA, J., PING, D. and DONG, X. **“Recent Developments of Graphene Oxide-based Membranes: A Review”** (2017). Membranes, 7, 52.

MARASCHIN, T. G. **“Preparação de oxido de grafeno e oxido de grafeno reduzido e dispersão em matriz polimérica biodegradável”** (2016). Pontificia Universidade Católica-RS, Porto Alegre.

MORAES. S.; BOTAN. R.; LONA. L. M. F. **“Synthesis and characterization of polystyrene/layered hydroxide salt nanocomposites”** (2013). Artigo do Departamento de Engenharia de Materiais e de Bioprocessos – Universidade Estadual de Campinas, Campinas.

MUÑOZ, P. A. R, et al. **“Novel improvement in processing of polymer nanocomposite based on 2D materials as fillers”** (2018). Express polymer letters, vol. 12, n. 10, 930-945.

NAFICY, S. JALILI, R. et al. **“Graphene oxide dispersions: tuning rheology to enable fabrication”** (2014). Materials Horizons, 1, 326-331.

NEGRETI, M. A. P. **“Obtenção e caracterização de compósitos poliméricos com óxido de grafeno reduzido”** (2016). Universidade de São Paulo, São Paulo.

NIU, R.; GONG, J.; XU, D.; TANG, T. and SUN, Z. **“Relationship between structures and rheological properties of plate-like particle suspensions”** (2015). Elsevier, Colloids and Surfaces A: Physicochemical and Engineering Aspects, 22-30.

OLIVEIRA, Y. D. C. **“Estudo da influência dos procedimentos de síntese do óxido de grafeno e do processamento na obtenção de nanocompósitos de polipropileno”** (2019). Universidade Presbiteriana Mackenzie, São Paulo.

OLIVEIRA, Y. D. C., AMURIN, L. G., VALIM, F. C. F., FECHINE, G. J. M. and ANDRADE, R. J. E. **“The role of physical structure and morphology on the photodegradation behaviour of polypropylene-graphene oxide nanocomposites”** (2019). Elsevier, Polymer, 176, 146-158.

OSHIMA, M. **“Efeitos farmacológicos e morfológicos do polietilenoglicol (peg 400) em preparações neuromusculares”** (2008). Dissertação de mestrado do curso de ciências médicas – UNICAMP, Campinas.

PINTO, E. P., RAMOS, G. Q., FILHO, H. D. F. **“O microscópio de força atômica (AFM): importante ferramenta no estudo da morfologia de superfícies na escala nanométrica”** (2013). Macapá, v. 3, n. 2, p. 41-50.

RICHARDSON, S. M. **“Now-Newtonin Fluids”** (2011). Thermopedia.

SAMPAIO, T. P. **“Obtenção e caracterização de óxido de grafeno e óxido de grafeno reduzido”** (2017). Universidade Federal de Pelotas, Pelotas.

SANTOS, W. O. **“Partição de β -galactosidase em sistemas aquosos bifásicos constituídos por polietileno glicol e poliacrilato de sódio”** (2011). Dissertação de mestrado do curso de engenharia de alimentos - Universidade Estadual do Sudoeste da Bahia, Bahia.

TAHA-TIJERINA, J. J. **“Thermal Transport and Challenges on nanofluids performance”** (2018). IntechOpen, Chapter 9.

TESFAI, W., SINGH, P., SHATILLA, Y., IQBAL, M. Z. and ABDALA, A. A. **“Rheology and microstructure of dilute graphene oxide suspension”** (2013). J. Nanopart Res, vol. 15, pp. 1989–1996.

THANGAVEL, S. and VENUGOPAL, G. **“Understanding the adsorption property of graphene-oxide with different degrees of oxidation leves”** (2014). Elsevier, Powder Technology, 257, 141-148.

VALIM, F. C. F. **“Comportamento reológico de compósitos reforçados com óxido de grafite em matriz poi(metracrilato de metila)”** (2015). Dissertação da escola politécnica – USP, São Paulo.

VASQUEZ, A. M. A. **“Estudo das propriedades reológicas de polipropilenos em fluxos de cisalhamento e fluxos elongacionais”** (2007). Dissertação de mestrado do curso de engenharia de materiais – Universidade de São Paulo, São Paulo.

VASU, K.S., KRISHNASWAMY, R., SAMPATH, S. and SOOD, A. K. **“Yield stress, thixotropy and shear banding in a dilute aqueous suspension of few layer graphene oxide platelets”** (2013). Soft Matter, vol. 9, pp. 5874–5882.

VIANNA, P. G. **“Nanocompósito de óxido de grafeno e nanopartículas metálicas para espectroscopia Raman Amplificada por Superfície (SERS)”** (2017). Universidade de Mackenzie, São Paulo.

VIEIRA SEGUNDO J. E. D. and VILAR, E. O. **“Grafeno: Uma revisão importante sobre propriedades, mecanismos de produção e potenciais aplicações em sistemas energéticos”** (2016). Revista eletrônica de materiais e processos, v.11, n. 2, 54-57.

WANG, C.; FENG, L., YANG, H.; XIN, G.; L.I. W., ZHENG, J.; TIAN, W. and LI, X. **“Graphene oxide stabilized polyethylene glycol for heat storage”** (2012). Phys. Chem. Chem. Phys, 14, 13233-13238.

WICK, P., LOUW-GAUME, A. E., KUCKI M, KRUG, H. F., KOSTAREOS, K.; et al. **“Classification Framework for Graphene-Based Materials”** (2014). Angewandte Chemie International Edition, Wiley- VCH Verlag, vol. 53 (n° 30), pp.7714-7718.

YU, W., DAS S.K, CHOI, S.U, PRADEEP, T. **“Nanofluids: Science and Technology”** (2007). Hoboken, NJ, USA: John Wiley & Sons, 416 p.

YU, W., XIE, H. and BAO D. **“Enhanced thermal conductivities of nanofluids containing graphene oxide nanosheets”** (2010). Nanotechnology, 21, 055705.

ZHANG, J. et al. **“Liquid Crystals of Graphene Oxide: A Route towards solution-based processing and applications”** (2017). Advanced Science News.

ZHONG, Y. ZHEN, Z. and ZHU, H. **“Graphene: fundamental research and potential applications”** (2017). Elsevier, FlatChem, 4, 20-32.

ZHU, Y., MURALI, S., CAI, W., LI, X., SUK, J.W., POTTS, J.R. **“Graphene and graphene oxide: synthesis, properties, and applications”** (2010). Adv Mater, vol. 22, pp. 3906–24.